[AMERICAN JOURNAL OF SCIENCE, VOL. 277, NOVEMBER, 1977, P. 1073-1123]

American Journal of Science

NOVEMBER 1977

MINERALOGY AND PETROLOGY OF THE INTRUSIVE COMPLEX OF THE PLINY RANGE, NEW HAMPSHIRE

GERALD K. CZAMANSKE*, DAVID R. WONES**, and JOHN C. EICHELBERGER***

ABSTRACT. Field relations, major-element analyses of rocks, and microprobe analyses of minerals from the Pliny Range, N.H. suggest that the rock units represent at least four phases of igneous activity. In chronological order, from oldest to youngest, the groups are: (1) coarse syenite and medium-grained syenite; (2) diorite and quartz monzodiorite; (3) porphyritic quartz monzonite, pink biotite granite, granite porphyry, and hastingsite quartz syenite; and (4) hastingsite biotite granite and Conway granite. The two older syenites are assigned to the White Mountain Magma Series of Mesozoic age, although they could be late Paleozoic in age.

The atomic ratio, Fe/(Fe+Mg), for the rocks ranges from 0.58 (diorite) to 0.98 (hastingsite quartz syenite); Fe/(Fe+Mg) of biotites ranges from 0.31 (medium-grained syenite) to 0.95 (Conway granite). Both whole-rock and biotite Fe/(Fe+Mg) ratios reflect the complex magmatic history and imply significant variation in oxidation state of the separate magmas. Other support for a complex history comes from details of amphibole chemistry, the F contents of amphiboles and biotites, and the Mn contents of ilmenites. These and other data preclude a genetic model based on continuous differentiation of a single parent magma. The complex chemical relations documented in these rocks seem best explained by different levels (and times?) of fusion for the magmas. Among these levels, the rocks may have been quite heterogeneous, as the Pliny Range intrusive rocks were emplaced within the Bronson Hill anticlinorium, a region of very complicated geologic and intrusive history.

INTRODUCTION

The syenite bodies of the Pliny Range are unique among the plutonic masses of New England for their large size and apparent older age. John Eichelberger mapped the area and investigated the structural and temporal relations of the syenites to the other rocks of the Pliny Range as a Master's thesis at Massachusetts Institute of Technology with David Wones. Subsequently, Gerald Czamanske determined the compositions of the mafic silicate and opaque oxide phases of the Pliny Range intrusive units and, with Wones, interpreted the conditions of crystallization and magmatic evolution of this intrusive complex.

The Pliny Range (fig. 1) occupies the northern third of the Mt. Washington Quadrangle, N.H. Its topography is closely related to the intrusion of stocks and ring dikes into an older (Highlandcroft) dome of plutonic and metavolcanic rocks. Outcrops are poor, and the best exposures are confined to the crest of the range and radial ridges.

* U.S. Geological Survey, Menlo Park, California 94025
** U.S. Geological Survey, Reston, Virginia 22092
*** Geosciences Group, Los Alamos Scientific Laboratory, University of California, Los Alamos, New Mexico 87544

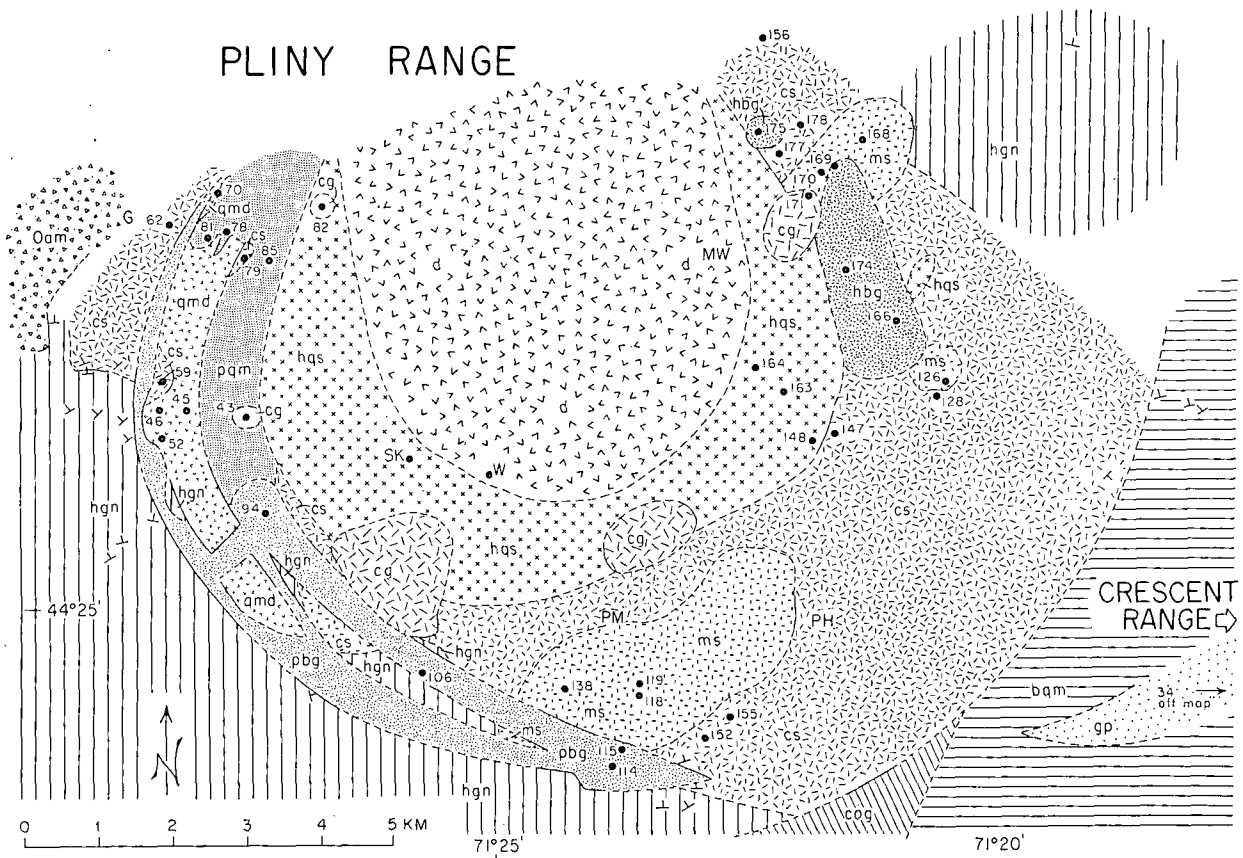

Fig. 1. Geologic map of Pliny Range, N.H., showing sample locations. See figure 2 for key to unit name abbreviations and intrusive relations. Geographic localities are as follows: G — Gore School; P — Pond Hill; PM — Pliny Mountain; SK — Mt. Starr King; W — Mt. Waumbek; MW — Mt. Weeks.

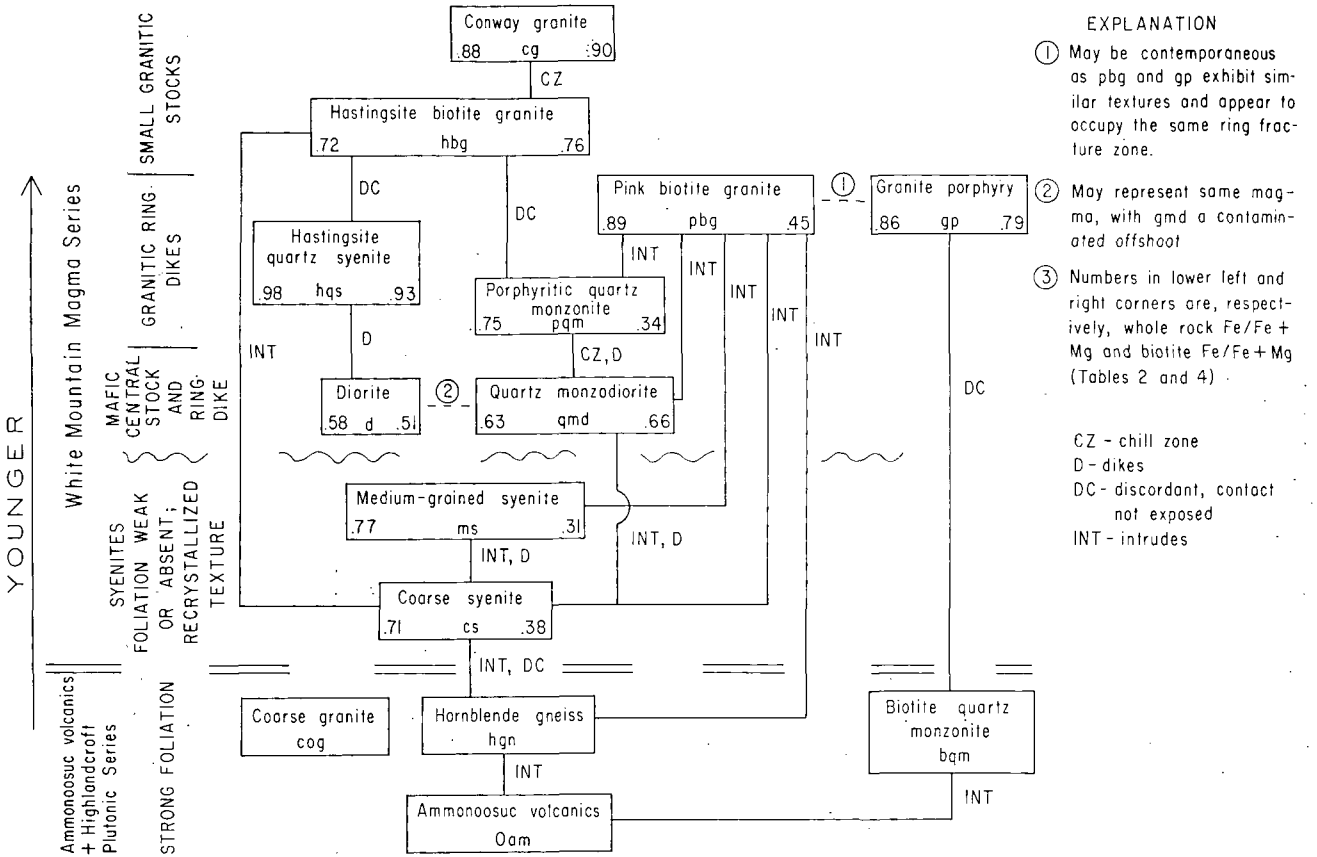

Fig. 2. Intrusive relations at the Pliny Ridge, N.H.

R. W. Chapman (1942) produced a geologic map and detailed description of the petrography and mineralogy of the units. Since that time, logging activity has made new exposures of bedrock. The present study began with remapping of the area on a scale of 1:62,500, using Chapman's map and stratigraphy as a guide. Most positions were located by use of an altimeter. Representative samples of the several rock units were selected for modal and bulk chemical analysis and for microprobe analysis of constituent mineral phases. Despite substantial modal variation within individual units, mafic mineral chemistry within each unit is distinctive.

GEOLOGY AND PETROGRAPHY

Nomenclature and age relationships

The rocks of the Pliny Range fall into four groups, the Ammonoosuc Volcanics, the Highlandcroft Series, the syenites, and the younger rocks of White Mountain Magma Series. Ammonoosuc Volcanics occur only as a tiny patch in the northwest corner of the area. Highlandcroft rocks, which crop out in the Bronson Hill anticlinorium, lie mostly outside the Pliny complex.

Rock nomenclature and age relations are summarized in figure 2. Few changes have been made to the rock names used by Chapman (1942). Modal and whole-rock chemical analyses of a sample from the central stock show that it is diorite, not quartz diorite, and quite distinct from the mafic ring dike of quartz monzodiorite. Mapping during the present study revealed two new units: a medium-grained syenite and a porphyritic quartz monzonite, both previously mapped as coarse syenite. Chapman's term pink biotite granite was retained to describe a complex ring dike rich in xenoliths which covers a much larger area than the "shatter zone" of the earlier map. Finally, the term "hornblende gneiss" is substituted for "hornblende quartz monzonite" because the former is more descriptive of the rock's texture. The gneiss is part of the Highlandcroft Series, presumed to be equivalent to the Oliverian Magma Series (Billings, 1956), and shown by Naylor (1969) to be of Ordovician age.

The two syenites have nearly identical textures and compositions. Chapman, Billings, and Chapman (1944) assigned the coarse syenite to the Oliverian Magma Series (OMS) on the basis of similarity of alkali feldspar phenocrysts in the syenite to megacrysts in the hornblende gneiss and on the belief that the syenite was similarly foliated. The coarse syenite is a smaller body than Chapman (1942) considered it to be, and some foliated rocks rich in alkali feldspar that are shown as coarse syenite on earlier maps are, in fact, porphyritic phases of the hornblende gneiss. The coarse syenite is in sharp contact with the hornblende gneiss, clearly truncates the foliation of the gneiss in some areas, and contains rounded inclusions of biotite gneiss and angular inclusions of hornblende gneiss. Both types of inclusions are disoriented with respect to the regional foliation and lineation. The coarse syenite has a weak primary foliation which sometimes parallels that of the Highlandcroft rocks.

The syenites clearly postdate the multiple deformations that have affected the Highlandcroft rocks. Furthermore, there are no units compositionally similar to the syenites among the "unstratified core rocks" (Naylor, 1969) of other Oliverian domes.

The syenites must be older than the non-orogenic White Mountain Magma Series (WMMS), because they show pervasive evidence of metamorphism in the form of recrystallization along grain boundaries. Page (1968) has suggested that there was a late Devonian, post-tectonic period of igneous activity in New England. Plutons thought to be of this age lack the foliated texture of the Highlandcroft and some plutons of the New Hampshire Magma Series (NHMS) but are older than the WMMS. The syenites may belong to such a group, but their structure, composition, and petrographic features are characteristic of the WMMS as defined by Billings (1956). Foland and Faul (1977) show that WMMS magmatic activity is as old as 235 m.y. and report an age of 188 ± 5 m.y. for the hastingsite biotite granite of the Pliny Range. Thus, the syenites could have been emplaced 40 m.y. before the younger syenites and still be a part of WMMS plutonism.

Although many of the age relations among WMMS units are firmly established (fig. 2), some ambiguities remain. These can be largely resolved by making a few attractive but not necessarily valid assumptions. The diorite and quartz monzodiorite appear to be closely related (for example, figs. 2, 3, and 4), and we judge that they were emplaced at about the same time. The quartz monzodiorite ring dike is clearly the earliest of the ring dikes, and the diorite may also be older than the other ring dikes. The pink biotite granite and granite porphyry are similar in texture and in position within the complex, so these ring dikes may have been emplaced at about the same time. Similarity of position, texture, composition, and style of intrusion suggests a close relation between the Conway granite and hastingsite biotite granite which represent the closing phase of activity in the Pliny Range. By analogy to caldera complexes of similar scale (Smith and Ross, 1961 and Smith, 1970), the Conway granite and hastingsite biotite granite may be the roots of rhyolite domes intruded around the ring fracture zone subsequent to caldera collapse and ring dike formation. Thus the intrusive sequence is most probably as given in figure 2. Note that the time of intrusion of the hastingsite quartz syenite can only be fixed between the time of intrusion of the dioritic units and the hastingsite biotite granite.

Description of the White Mountain Magma Series units

In order to lead the reader more directly through the paper, detailed petrographic descriptions of the rock units are presented as an appendix; modal analyses and some mineralogic data are given in table 1; and crystallization sequences are interpreted in figure 3. The brief descriptions in the following paragraphs and the appendix should be supplemented by the more balanced descriptions of Chapman (1942) who also provides additional quantitative microscopic data for mineral phases.

TABLE 1

Modes, in volume percent,* of intrusive rocks of the Pliny Range, N.H., with additional data for mineral species

Rock Type	Specimen Number	Quartz	Alkali Feldspar	Plagioclase Feldspar	Pyroxene	Amphibole	Biotite	Chlorite	Opaques	Sphene
Coarse Syenite	CS-59	2.7	63.8	27.9 (m-23; ex-24)**	-	2.1 (1.672)***	1.6	-	1.2	0.7
	CS-62	1.3	79.8	11.7 (p-25'; m-26; ex-26)	-	-	4.0	-	2.1	1.1
	CS-79	4.4	67.7 (74)†	14.5 (m-24; ex-24)	-	9.1 (1.712)	0.8	0.5	0.4	3.6
	CS-123	6.9	57.9 (74)	25.8 (p-29'; m-26)	-	1.6 (1.688)	5.7 (1.616)[2]	-	0.6	1.5
	CS-147	0.8	67.0	20.3 (m-22')	-		10.9 (1.634)	0.5	0.4	0.2
	CS-152	9.6	56.6	23.8 (m-12; ex-11)	-	4.6 (1.684)	4.3 (1.684)	0.3	0.2	0.6
	CS-156	14.7	47.3	34.6 (p-24; m-24)	-	0.5 (1.681)	1.3 (1.614)	-	0.2	0.9
	CS-178	10.3	43.8 (76)	39.5 (c-50; p-26; m-26)	-	3.4 (1.686)	-	1.4	0.9	0.7
Medium-Grained Syenite	MS-118	6.3	74.5 (63)	16.0 (c-29; p-25; m-20; ex-16)	-	0.3 (1.675)	1.2 (1.623)	0.8	1.6	0.2
	MS-138	8.4	63.1 (62)	23.8 (m-23; ex-17)	-	tr	2.4 (1.619)	0.1	1.2	1.0
	MS-126	8.0	67.2	18.8	-	-	-	4.0	2.0	tr
	MS-168	7.0	41.0	49.0 (p-15; m-11; ex-7)	-	-	-	0.9	0.6	1.5
	MS-170	22.0	44.6	30.4 (p-15'; m-8; ex-8)	-	-	-	1.2	1.3	0.6
Diorite	D-W	0.9	3.3	57.8 (c-54; r-23)	5.7	12.9 (1.671)	8.2 (1.658)	7.4	3.5	0.3
Quartz Monzo-Diorite	QMD-45	5.3	12.4	55.2 (c-48; r-23)	0.8	6.5 (1.694)	13.3 (1.670)	5.0	1.0	-
	QMD-46	5.4	25.7 (68)	43.0 (c-45; r-24)	-	12.0 (1.723)	10.1 (1.677)	0.5	3.3	-
	QMD-52	9.4	12.0	42.6 (c-62; r-21)	0.9	10.1 (1.696)	24.0 (1.682)	0.3	0.6	-
	QMD-70	6.7	1.5	53.7 (c-47; r-23)	-	19.8	13.9	-	4.4	0.5
Hastingsite Quartz Syenite	MHG-SK	20.1	51.9 (55)	24.9 (p-28; ex-10)	-	-	-	-	2.3	0.3
	MHG-148	15.4	64.6	16.0 (c-17'; r-13; ex-13)	-	-	0.2	-	1.4	0.5
	MHG-163	16.3	57.5	22.3 (c-17'; r-10; ex-8)	-	3.0 (1.730)	0.2	-	1.0	-
	MHG-164	17.7	73.7 (52)	2.4 (c-27'; r-18'; ex-7)	-	5.0 (1.728)	0.1	-	1.0	-

Porphyritic	PQM-78	24.2	27.2	41.4 (p-18'; m-20')	-	3.0	1.2	-	1.2	1.4
Quartz	PQM-81		(68)			(1.669)	(1.633)	-	-	-
Monzonite	PQM-85	24.9	34.9 (59)	36.6 (p-18'; m-18; ex-7)	-	0.1	2.3 (1.626)	-	0.9	0.3
Pink	PBG-94	42.8	27.7 (80)	24.5 (m-23)	-	0.2 (1.663)	3.6 (1.636)	0.3	0.7	0.3
Biotite	PBG-106	11.1	58.7	26.7 (m-25)	-	-	0.8 (1.636)	0.4	1.3	0.4
Granite	PBG-114	30.5	43.3 (68)	23.7 (m-26)	-	-	0.4 (1.637)	0.3	1.0	0.8
Granite Porphyry	GP-34	39.9	49.6 (60)	5.8 (c-27'; p-23; m-10)	-	1.7 (1.715)	0.8 (1.675)	1.4	0.9	-
Hastingsite	HBG-166	20.9	56.7	18.1 (m-10; ex-9)	-	0.9 (1.713)	2.4 (1.676)	-	0.9	0.1
Biotite	HBG-169	31.7	36.6	26.2 (c-35'; m-25)	-	-	4.7	-	0.5	0.3
Granite	HBG-174	16.1	45.0 (67)	34.7 (m-13; ex-7)	-	-	2.8 (1.670)	-	1.1	0.3
	HBG-175	31.6	42.8	21.6 (m-11)	-	tr (1.710)	3.5 (1.672)	-	0.2	0.3
Conway	CG-43	30.2	41.9	21.5 (p-9; ex-9')	-	-	0.1	-	0.3	-
Granite	CG-82	33.2	61.3	4.8 (p-12)	-	1.1 (1.727)	tr (1.684)	-	-	-
	CG-171	31.7	47.3 (74)	18.7 (p-10; ex-10')	-	0.3 (1.725)	1.4 (1.684)	-	0.3	0.1

*Modes based on 1000 counts per thin section, one thin section per sample.

**Plagioclase compositions in mole percent An as determined by extinction angle measurement on universal stage:

c - core; represents core of plagioclase grain if associated with "r", otherwise plagioclase core in perthite.

r - rim; represents margin of plagioclase grain.

p - phenocryst; represents large plagioclase grain in porphyritic rock.

m - matrix; represents plagioclase in groundmass of porphyritic rock.

ex - exsolution; represents plagioclase phase of perthite.

' - denotes single determination, remaining values are averages of 2-3 determinations.

***Value in parentheses is refractive index γ, for primary amphibole, determined with sodium light.

†Value in parentheses is weight percent Or determined by X-ray on homogenized alkali feldspar (201, 850°C, 1/2 kb, 5 days; Wright, 1963).

Further descriptive information for these and the older rock units also can be found in Eichelberger (ms). Our descriptions emphasize observations based on the mapping of the units and details of their mafic mineral assemblages. We provide the first published chemical analysis and CIPW norms for these rocks in table 2.

Coarse syenite.—The coarse syenite ranges from coarse to very coarse grained. Pink perthite phenocrysts, up to 2 cm long, commonly exhibit Carlsbad twins and contain magnetite inclusions. They are accompanied by smaller and less abundant plagioclase phenocrysts. Major constituents of the matrix are quartz, plagioclase, perthite, amphibole, biotite, sphene,

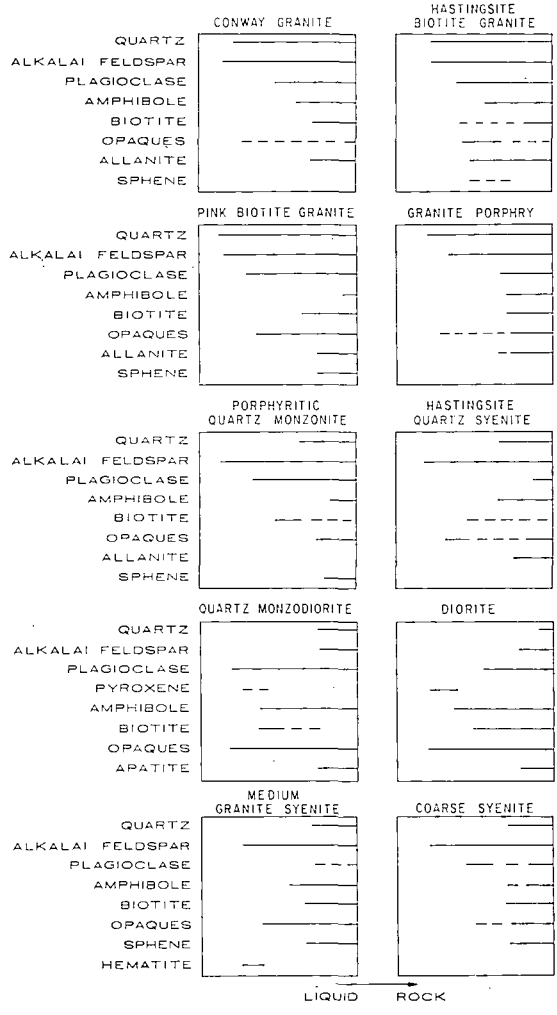

Fig. 3. Approximate sequences of crystallization in the rock units of the Pliny Range, N.H.

and magnetite. Although the unit is not homogeneous, no systematic variations were discerned.

Medium-grained syenite.—The medium-grained syenite is more resistant to erosion than the coarse syenite and forms low cliffs on the south side of Pliny Mountain. Its greater homogeneity, smaller grain size, and lower mafic content distinguish it from the coarse syenite. In hand specimen the rock appears to consist entirely of alkali feldspar, except for scattered blotches of fine-grained mafic minerals. The rock is pale pink, approaching pale red-purple, and is more uniformly colored than the coarse syenite.

Near the north end of the central stock of medium-grained syenite, at about 800 m elevation, there is a spectacular igneous breccia involving 2-m blocks of typical coarse syenite that are suspended and disoriented in medium-grained syenite. Elsewhere, as in the saddle just west of Pond Hill and southward, large boulders of coarse syenite contain dikes of medium-grained syenite.

Medium-grained hastingsite biotite granite is similar in gross appearance to the medium-grained syenite, but the former weathers to a distinctive rusty pink, has more quartz, and has sharply defined hornblende and magnetite grains, rather than blotches of fine mafic minerals. The granite, unlike the syenite, usually shows miarolitic cavities and seams.

Diorite and quartz monzodiorite.—Diorite and quartz monzodiorite (figs. 3 and 4) are the darkest of the non-foliated rocks and contain about one-third mafic minerals. Each rock type is quite uniform in hand specimen except for minor variations in grain size from medium to coarse, and they are not easily distinguished. The stock contains little quartz and alkali feldspar (W, table 1) and is a true diorite. Miarolitic cavities containing quartz crystals are commonly found in the ring dike.

At the north end of the ring dike, a few small, rounded inclusions of coarse syenite were observed. Four hundred meters west of the ring dike, a 30-cm-wide dike of quartz monzodiorite, striking radially to the main dike, cuts both the hornblende gneiss and the coarse syenite. The presence of the older coarse syenite between the ring dike and the central stock shows that the ring dike is a separate structure and is not a fragment of the stock that became detached by later intrusions or by faulting.

Hastingsite quartz syenite.—This unit, the largest and most resistant ring dike, underlies the main crest of the Pliny Range. The rock is homogeneous through the 14-km length of the ring dike and contains few inclusions. It is generally orange-pink, the color of its predominant constituent, perthite. Quartz crystals are clear, prominent, and confined to the interstices. Hornblende is unaltered and subhedral; biotite is scarce.

Prominent features of the rock are abundant veins and miarolitic cavities containing quartz crystals and some euhedral magnetite. Around the summits of Mounts Waumbek and Weeks, near the contact of the central diorite stock and the hastingsite quartz syenite, the diorite con-

tains numerous small dikes which are interpreted as offshoots of the hastingsite quartz syenite.

Porphyritic quartz monzonite.—This unit was not recognized by Chapman (1942) who may have considered it to be coarse syenite. Field relations clearly preclude that possibility, and the unit is chemically (tables 2 and 3) and modally (table 1) distinct. Porphyritic quartz monzonite occupies most of the area adjacent to the concave side of the quartz monzodiorite ring dike and truncates it at its north end. The unit is well exposed only on the ridge east of Gore School, near the northern end of the ring dike. Texture and composition are uniform throughout the body.

The quartz monzonite is similar to the coarse syenite in appearance because of its large pink phenocrysts, but its alkali feldspar is a more intense pink, and it contains abundant quartz in small shattered aggregates. As in the syenites, mafic minerals are fine grained and occur in clots.

A dike of porphyritic quartz monzonite, 33 m wide, intrudes the north end of the quartz monzodiorite ring dike. This contact is exposed

TABLE 2

Analyses* and CIPW** norms for rocks from the Pliny Range, N.H.

	Coarse Syenite	Medium-grained Syenite	Diorite	Quartz Monzo-diorite	Hastingsite Quartz Syenite	Porphyritic Quartz Monzonite	Pink Biotite Granite	Granite Porphyry	Hastingsite Biotite Granite	Conway Granite
Sample Number	177	119	W	70	SK	78	115	34	169	171
SiO_2	64.4	65.5	50.1	54.1	69.3	69.3	74.5	72.1	73.0	72.7
Al_2O_3	18.1	17.5	15.6	16.5	14.7	15.6	13.0	13.9	13.5	14.4
Fe_2O_3	1.60	1.56	3.37	1.80	3.39	1.75	1.34	0.94	0.29	0.91
FeO	1.00	0.93	8.25	7.72	1.40	0.91	0.44	1.29	1.34	1.18
MgO	0.55	0.40	4.6	3.1	0.05	0.47	0.11	0.20	0.34	0.15
MnO	0.03	0.06	0.20	0.20	0.02	0.03	0.00	0.08	0.03	0.04
TiO_2	0.43	0.28	2.9	2.5	0.31	0.30	0.16	0.29	0.31	0.22
CaO	2.0	1.2	7.1	5.8	0.29	1.4	0.50	0.82	0.89	0.61
Na_2O	4.91	5.37	3.67	3.68	5.47	4.50	3.30	4.35	3.82	4.02
K_2O	6.43	6.58	2.35	3.53	4.37	5.51	5.60	5.14	5.12	5.41
P_2O_5	0.13	0.06	0.56	0.82	0.02	0.07	0.00	0.04	0.05	0.00
F	0.06	0.03	0.08	0.12	0.03	0.01	0.02	0.05	0.08	0.01
H_2O^+	0.92	0.75	1.1	1.3	0.54	0.76	0.72	0.81	0.63	0.13
Total	100.56	100.22	99.88	101.17	99.89	100.61	99.69	100.01	99.40	99.78
Q	6.69	6.37	--	1.59	20.23	18.51	32.80	24.81	28.52	26.66
C	--	--	--	--	0.57	--	0.66	--	0.38	0.85
OR	37.79	38.80	13.90	20.62	25.85	32.36	33.20	30.37	30.44	32.04
AB	41.32	45.34	31.09	30.78	46.34	37.85	28.01	36.81	32.52	34.09
AN	8.31	4.20	19.18	17.87	1.10	6.06	2.34	3.22	3.56	2.96
WO	0.15	0.49	5.10	2.06	--	0.15	--	0.10	--	--
EN	1.36	0.99	7.92	7.63	0.13	1.16	0.28	0.50	0.85	0.37
FS	--	0.07	5.49	8.83	--	--	--	1.26	1.78	1.13
FO	--	--	2.49	--	--	--	--	--	--	--
FA	--	--	1.90	--	--	--	--	--	--	--
MT	2.06	2.26	4.89	2.58	3.68	2.15	0.96	1.36	0.42	1.32
HM	0.17	--	--	--	0.85	0.26	0.68	--	--	--
IL	0.81	0.53	5.51	4.69	0.59	0.57	0.31	0.55	0.59	0.42
AP	0.31	0.14	1.33	1.92	0.05	0.17	--	0.10	0.12	--
FR	0.10	0.05	0.06	0.10	0.06	0.01	0.04	0.10	0.16	0.02
SALIC	94.10	94.71	64.17	70.86	94.09	94.78	97.01	95.20	95.41	96.60
FEMIC	4.96	4.53	34.70	27.81	5.36	4.46	2.26	3.97	3.92	3.27
(Na+K)/Al	0.83	0.91	0.55	0.60	0.93	0.86	0.88	0.92	0.88	0.87
(Na+K+Ca)/Al	0.93	0.97	0.96	0.92	0.95	0.94	0.92	0.97	0.94	0.90
Na/(Na+K)	0.54	0.55	0.70	0.61	0.66	0.55	0.47	0.56	0.53	0.53
Fe^{+3}/Fe^{+2}	1.45	1.50	0.37	0.21	2.18	1.73	2.75	0.65	0.19	0.69
Fe/(Fe+Mg)	0.71	0.77	0.58	0.63	0.98	0.75	0.89	0.86	0.72	0.88

*Fe_2O_3 colorimetrically with orthophenanthroline; FeO volumetrically with dichromate; Na_2O, and K_2O by flame photometer: all by M. Cremer, USGS; remaining elements by wet chemical, rapid-rock techniques in the USGS laboratory of L. Shapiro.

**Calculated by USGS computer program C542 (Bowen, 1971).

on a low cliff a few yards south of the col that lies between the minor summit 1.6 km east of Gore School and the main ridge. This was the only place in the Pliny Range where the dip of a contact was observed. The contact is sharp and regular, dips 50° toward the center of the Pliny complex, and strikes parallel to the other ring dike contacts; a cone sheet is suggested.

Pink biotite granite.—The pink biotite granite is the matrix of a ring dike strikingly different from the other dikes, as it is an igneous breccia through most of its length. The only exposure observed in which the matrix predominates over the inclusions is at the eastern end of the dike on Pliny Mountain. Despite the high content of xenoliths, the granite matrix is surprisingly homogeneous, although less so than the other ring dikes. It is medium grained and usually equigranular. Pink perthite contrasts strongly with white plagioclase, clear quartz, and dark biotite.

Miarolitic cavities containing quartz and biotite crystals are common in association with pegmatite areas. The pegmatites do not occur as dikes but as blotches grading into the surrounding rock; they consist largely of intergrown perthite and quartz with crystals as much as 5 cm across.

In the southwest part of the ring dike, the xenolithic material is entirely hornblende gneiss. Southwest of Mt. Starr King and east of the screen of hornblende gneiss, the inclusions are all coarse syenite. Slightly farther southwest, where the granite truncates the quartz monzodiorite ring dikes, the inclusions are quartz monzodiorite. Along the thin dike that circles the west rim of the range, there is a jumble of hornblende gneiss, coarse syenite, and quartz monzodiorite to the south and coarse syenite, quartz monzodiorite, and a little prophyritic quartz monzonite to the north. Thus, if one disregarded the matrix and mapped the xenoliths as bedrock, the map pattern would not be changed except for the removal of the unit of pink biotite granite. This pattern and the angularity of the xenoliths indicate that the inclusions were not transported far but rather were engulfed in the rising granitic magma. The concept is implied by Chapman's (1942) term, "shatter zone," for the structure.

Granite porphyry.—The pink biotite granite ring dike appears to pinch out south of Pliny Mountain but, if extended, would pass smoothly into the granite porphyry ring dike that forms the Crescent Range. This fact and the similarity of a minor porphyritic phase of pink biotite granite to the granite porphyry suggest that these two units might be the product of a single magma and perhaps a single intrusive event. An unsuccessful search was made to find connecting dikes or faults.

The granite porphyry is grayish orange-pink. The subdued color is due to the small grain size of the mafic minerals in the very fine groundmass. It is the only unit containing quartz phenocrysts apart from rare examples in the pink biotite granite.

TABLE 3

Electron microprobe analyses and ions per 23 oxygen atoms for

Rock Name	Coarse Syenite		Medium-Grained Syenite	Diorite		Quartz Monzodiorite		Hastingsite Quartz Syenite
Specimen Number	155(2) *	178(2)	138(2)	W_1(1)**	W_2(2)	46_1(3)	46_2(2)	165(1)
	◆	◆	◆	◘	◘	■	◆	×
SiO_2	41.9 (.5)***	42.1 (.6)	49.2 (.6)	46.5 (.5)	41.8 (.6)	41.0 (.5)	39.6 (.6)	39.8 (.7)
Al_2O_3	10.6 (.3)	10.1 (.4)	5.22(.13)	6.57(.17)	10.7 (.4)	8.94(.3)	8.91(.5)	7.80(.4)
$FeO^{\dagger}$	20.3 (.3)	19.7 (.3)	12.8 (.4)	17.5 (.6)	15.8(1.3)	25.2 (.4)	28.5 (.4)	32.1 (.3)
$Fe_2O_3^{\dagger\dagger}$	6.88	6.88	4.34	5.94	5.36	8.55	9.67	10.9
$FeO^{\dagger\dagger}$	14.1	13.69	8.89	12.2	11.0	17.5	19.8	22.3
MgO	9.01(.2)	9.63(.2)	14.8 (.3)	12.0 (.4)	10.8 (.9)	5.39(.4)	5.96(.2)	0.87(.09)
MnO	0.61(.02)	0.97(.04)	0.90(.05)	0.41(.03)	0.31(.03)	0.83(.03)	0.72(.05)	1.11(.05)
TiO_2	0.42(.03)	0.35(.03)	0.97(.12)	1.85(.16)	3.89(.2)	2.68(.14)	0.59(.24)	1.71(.07)
CaO	11.5 (.2)	11.4 (.2)	11.5 (.2)	10.7 (.15)	11.2 (.2)	10.6 (.2)	11.0 (.3)	10.2 (.3)
Na_2O	1.69(.09)	1.93(.06)	1.86(.12)	1.66(.04)	2.37(.08)	2.10(.06)	1.66(.2)	2.25(.1)
K_2O	1.31(.06)	1.34(.08)	0.66(.05)	0.62(.04)	1.08(.05)	1.30(.11)	2.03(.2)	1.27(.05)
Cl	0.07(.02)†††	0.07(.02)	0.10(.05)	0.10(.03)		0.24(.04)	2.44(.22)	0.47(.06)
F	1.0 (.3)†††	0.9 (.2)	1.2 (.3)	0.3 (.2)		0.5 (.3)	0.3 (.2)	0.7 (.2)
Total	99.1	99.2	99.6	98.8	98.5	99.6	100.7	99.4
Si	6.36	6.38	7.13	6.86	6.20	6.33	6.30	6.40
Al	1.64	1.62	0.87	1.14	1.80	1.63	1.67	1.48
Fe^{3+}	0.00	0.00	0.00	0.00	0.00	0.04	0.03	0.12
Σ(tet.)	8.00	8.00	8.00	8.00	8.00	8.00	8.00	8.00
Al	0.26	0.19	0.02	0.00	0.08	0.00	0.00	0.00
Fe^{3+}	0.79	0.76	0.47	0.66	0.60	0.94	1.13	1.20
Fe^{2+}	1.79	1.74	1.08	1.50	1.37	2.26	2.64	3.00
Mg	2.04	2.18	3.20	2.64	2.39	1.24	0.94	0.21
Ti	0.05	0.10	0.11	0.20	0.43	0.31	0.07	0.21
Mn	0.08	0.04	0.11	0.00	0.04	0.11	0.10	0.15
$\Sigma(M_1\text{-}M_3)$	5.01	5.01	4.99	5.00	4.91	4.86	4.88	4.77
Ca	1.87	1.85	1.78	1.69	1.78	1.75	1.88	1.75
Mn	0.00	0.03	0.00	0.05	0.00	0.00	0.00	0.00
Fe^{2+}	0.00	0.00	0.00	0.00	0.00	0.00	0.00	0.00
Na	0.13	0.12	0.22	0.26	0.22	0.25	0.12	0.25
$\Sigma(M_4)$	2.00	2.00	2.00	2.00	2.00	2.00	2.00	2.00
Na	0.37	0.45	0.31	0.22	0.46	0.38	0.39	0.45
K	0.25	0.26	0.12	0.12	0.20	0.26	0.41	0.26
Σ(A)	0.62	0.71	0.43	0.34	0.66	0.64	0.80	0.71
Fe/Fe+Mg^^	0.56	0.53	0.33	0.45	0.45	0.72	0.80	0.95
Na/Na+K	0.67	0.69	0.82	0.80	0.77	0.71	0.55	0.73
F/Cl	26.3	23.7	22.6	5.6		3.9	0.23	2.9

*Number in parentheses is number of discrete amphibole grains represented by average oxide values listed.

**Listing of two analyses for a specimen indicates presence of at least two distinct amphibole compositions in rock.

***Value in parentheses is the greater of (a) the standard deviation for one of the individual analysis or (b) the spread between the average and the most extreme individual value.

* All Fe calculated as FeO.

amphiboles from the Pliny Range, N.H.

Hastingsite Quartz Syenite	Porphyritic Quartz Monzonite	Pink Biotite Granite	Granite Porphyry	Hastingsite Biotite Granite		Conway Granite		
164(3)	85(1)	94(3)	34(2)	166_1(2)	166_2(2)	82(3)	171_1(1)	171_2(2)
+	▲	△	▲	○	⊕	●	◑	◐
40.6 (.9)	48.4 (.6)	48.4 (.3)	41.7 (.5)	41.1 (.4)	39.8 (.6)	40.8 (.5)	40.4 (.7)	39.4 (.9)
6.77(.6)	5.92(.25)	5.87(.6)	6.94(.1)	7.79(.3)	7.92(.4)	6.61(.2)	7.67(.4)	7.95(.2)
32.2 (.9)	13.6 (.23)	14.1 (.3)	28.7 (.4)	27.7 (.4)	29.4 (.2)	33.0 (.3)	29.9 (.2)	31.1 (.6)
10.9	4.61	4.78	9.74	9.40	9.97	11.2	10.1	10.6
22.4	9.45	9.80	19.9	19.2	20.4	22.9	20.8	21.6
1.86(.5)	13.7 (.15)	13.9 (.2)	3.53(.1)	3.79(.3)	2.97(.05)	1.36(.05)	2.68(.2)	2.00(.2)
0.95(.06)	1.10(.01)	0.62(.03)	1.62(.1)	1.70(.15)	1.85(.05)	0.86(.03)	1.37(.06)	1.34(.07)
1.37(.3)	0.97(.10)	1.08(.1)	1.56(.1)	1.84(.2)	0.51(.13)	1.60(.15)	1.80(.2)	1.27(.5)
9.71(.2)	11.7 (.5)	11.9 (.08)	9.88(.1)	9.89(.2)	10.5 (.1)	9.77(.12)	9.64(.2)	10.2 (.14)
2.36(.1)	1.56(.08)	1.21(.1)	2.28(.1)	2.46(.1)	1.76(.13)	2.13(.08)	2.26(.08)	2.06(.1)
1.22(.05)	0.76(.03)	0.76(.04)	1.14(.06)	1.00(.05)	1.60(.05)	1.19(.06)	1.08(.04)	1.38(.1)
0.39(.06)	0.10(.02)	0.11(.03)	0.34(.06)	0.25(.03)	0.96(.07)	0.39(.05)	0.37(.05)	0.58(.15)
1.0 (.3)	0.6 (.2)	0.4 (.3)	1.0 (.3)	0.7 (.2)	0.5 (.3)	0.6 (.2)	0.6 (.2)	0.7 (.4)
99.5	98.9	98.8	99.6	99.1	98.7	99.4	99.0	99.1
6.52	7.06	7.04	6.58	6.47	6.42	6.54	6.43	6.35
1.28	0.94	0.96	1.29	1.45	1.51	1.25	1.44	1.51
0.20	0.00	0.00	0.13	0.08	0.07	0.21	0.13	0.14
8.00	8.00	8.00	8.00	8.00	8.00	8.00	8.00	8.00
0.00	0.08	0.05	0.00	0.00	0.00	0.00	0.00	0.00
1.11	0.51	0.52	1.02	1.03	1.13	1.14	1.08	1.15
3.01	1.15	1.19	2.63	2.53	2.75	3.07	2.77	2.91
0.44	2.98	3.02	0.83	0.89	0.71	0.32	0.68	0.48
0.17	0.11	0.12	0.19	0.22	0.06	0.19	0.22	0.15
0.13	0.14	0.08	0.22	0.23	0.25	0.12	0.18	0.18
4.86	4.97	4.98	4.89	4.90	4.90	4.84	4.93	4.87
1.67	1.83	1.86	1.67	1.67	1.81	1.68	1.64	1.76
0.00	0.00	0.00	0.00	0.00	0.00	0.00	0.00	0.00
0.00	0.00	0.00	0.00	0.00	0.00	0.00	0.00	0.00
0.33	0.17	0.14	0.33	0.33	0.19	0.32	0.36	0.24
2.00	2.00	2.00	2.00	2.00	2.00	2.00	2.00	2.00
0.40	0.27	0.20	0.37	0.42	0.36	0.34	0.34	0.40
0.25	0.14	0.14	0.23	0.20	0.33	0.24	0.22	0.28
0.65	0.41	0.34	0.60	0.62	0.69	0.58	0.56	0.68
0.91	0.36	0.36	0.82	0.80	0.85	0.93	0.85	0.90
0.74	0.76	0.79	0.75	0.79	0.63	0.73	0.76	0.70
4.8	11.3	6.8	5.5	5.2	9.97	2.9	3.0	2.4

†FeO value based on electron microprobe value for Fe.

††Values for partioned Fe^{3+} and Fe^{2+} based on wet chemical determination of 69.5 percent ferrous iron in 178.

†††Std. deviations based on statistics for 10-12, 20-second count intervals on distinct point areas, several grains. 10 KV, 20$\mu\alpha$, beam defocussed to 20 microns.

Total is for partitioned Fe_2O_3, FeO values.

Atomic ratios.

Hastingsite biotite granite.—The hastingsite biotite granite forms two small, poorly exposed stocks on the eastern slopes of the range. The smaller stock appears to intrude the outer rim of the hastingsite quartz syenite dike, and we believe it to be the younger unit. Isolation from other units of the series prevents establishment of direct age relations. Two factors suggest that it is younger than the pink biotite granite. (1) Its overall appearance is similar to the Conway granite, which seems to intrude the pink biotite granite ring dike (exposures are also poor in that area) and which elsewhere in New Hampshire is the youngest unit of the WMMS. (2) The style of intrusion, like that of the Conway granite, is as stocks rather than as ring dikes.

Conway granite.—Conway granite occurs in five small stocks surrounding the crest of the range and possibly in smaller ones that escaped observation. Except for the stock east of Mt. Weeks, none is well exposed. The Conway granite is similar to the hastingsite biotite granite. The rock is pale pink with flecks of biotite or amphibole. It is coarser grained, richer in quartz and alkali feldspar, and poorer in plagioclase than the hastingsite biotite granite. Quartz grains are subhedral, are not notably interstitial, and are prominent on weathered surfaces.

Map patterns indicate that the Conway granite intrudes the two syenites and all other WMMS units. In the only observed contact, the Conway granite is chilled against the hastingsite biotite granite.

CHEMISTRY OF THE MAFIC SILICATES AND Fe–Ti OXIDES

Analytical Procedures

For each reported analysis a grain or group of grains was separately analyzed three times for determination of the following groups of three elements, Fe, Ca, Mg; Ti, Si, Al; and Mn, K, Na. Typically 6 to 12 points were analyzed for each set of elements. Three selected silicate standards, an amphibole, a biotite, and a pyroxene, were used for the bulk of this study (for complete data on these standards and details of analytical method, see Czamanske and Wones, 1973).

For calculations of hydrous phase unit-cell occupancy for microprobe data, some (for example Borg, 1967; Gorbatschev, 1969; Robinson, Ross, and Jaffe, 1971) have considered it satisfactory to calculate structural formulae on the basis of a fixed number of oxygen atoms.

Ludington and Munoz (1975) and Ludington (1974) have suggested that when a complete analysis is unavailable, a biotite unit cell calculation based on seven octahedral and tetrahedral cations may be more rigorous than calculations based on 44 anionic charges (Foster, 1960) or 24 anions (Deer, Howie, and Zussman, 1962). This method assumes no vacancies in the octahedral cationic sites, and, if significant octahedral cations are not analyzed (Li being most likely to be missed), it will yield a mole fraction of the analyzed cations higher than the actual value. Using the assumption of electrostatic neutrality, this method also estimates the OH content. The structural formulae of table 4 and the value $Fe/\Sigma(M_1\text{-}M_2)$ of figure 9 are based on Ludington's scheme. The aluminum

balance between tetrahedral and octahedral sites is the most sensitive parameter to calculation scheme; the seven cation scheme produces higher site occupancy for Si and, consequently, higher octahedral site occupancy for Al.

Wet-chemical determinations of ferrous iron were made on an amphibole separate from coarse syenite specimen 178 (table 3) and on biotite separates from hastingsite biotite granite specimen 174 and Conway granite specimen 171 (table 4). Of the specimens used for microprobe study, only these three contained mafic silicate phases of such texture and abundance that pure separates could be obtained. For the amphibole from 178, 100 $FeO/(FeO+Fe_2O_3)$ is 69.5, in biotite from 174 it is 94.7, and in biotite from 171 it is 86.4. All the amphibole unit-cell data in table 3 have been calculated on the basis of 69.5 percent of total iron as ferrous, and most of the biotite unit-cell data of table 4 have been calculated on the basis of 90.5 percent of total iron as ferrous. (Exceptions to this are biotite analyses 171 and 174, for which the measured values were used.) In view of the different oxidation states of the Pliny Range magmas, this is clearly only a first approximation. We have tried to avoid injudicious use of mineral Fe^{+3}/Fe^{+2} ratios and discuss specific deficiencies in this approach as the analyses are considered. A great number of ferrohastingsite analyses (for example, Billings, 1928; Buddington and Leonard, 1953; Borley and Frost, 1963; Billings and Wilson, 1964) have ferrous iron contents equivalent to 79 to 83 percent of total iron. On the basis of this consideration and the fact that many of the Pliny Range units have values of Fe^{+3}/Fe^{+2} less than that of the medium-grained syenite (table 2), the estimate of ferrous iron percentage for the Pliny Range amphiboles is probably a minimum.

Amphiboles

Pliny Range amphiboles are unusually low in Al and high in Na for hastingsitic amphiboles (Deer, Howie, and Zussman, table 43). Found in a compositionally diverse suite of rocks, these amphiboles show substantial variation in Fe/(Fe+Mg), TiO_2, MnO, and Al_2O_3, although their structural formulae show consanguinity. The most notable characteristic of the amphiboles as a group are: (1) unusually high content of Fe; (2) low content of Al; (3) indication of a coupling between Ti and Na in the M_4 site; (4) the fact that second generation blue-green amphiboles in a given rock are less sodic and more Cl-rich than the primary amphibole; and (5) the suggestion that Fe^{+3} may enter the tetrahedral site.

The poor correlation between Fe/(Fe+Mg) for the amphiboles and Fe/(Fe+Mg) for the host rocks, as shown in figure 5, implies that intensive parameters varied substantially during crystallization of the Pliny Range rocks. Replacement of green by blue amphibole consistently involves decreases in SiO_2, MgO, TiO_2, and Na_2O contents and increases in FeO, CaO, K_2O, and Cl. There are no other systematic variations of amphibole composition with age or SiO_2 content of the rock units.

TABLE 4

Electron microprobe analyses and structural formulae based on

Rock Name	Coarse Syenite		Medium-Grained Syenite	Diorite	Quartz Monzo-diorite	Hastingsite Quartz Syenite	
Specimen Number	155(2)* ◆	147(2) ◇	138(2) ◆	W(2) ▭	46(3) ■	163(1)** ×	164(2) +
SiO_2	38.0 (.5)***	36.9 (.6)	39.7 (.5)	36.7 (.6)	35.5 (.2)	33.0 (.5)	33.4 (.7)
Al_2O_3	14.4 (.2)	14.7 (.3)	12.4 (.2)	13.3 (.2)	12.7 (.2)	11.3 (.1)	11.3 (.3)
FeO†	15.6 (.4)	16.4 (.4)	13.7 (.4)	20.1 (.5)	25.7 (.4)	33.5 (.4)	34.7 (.4)
Fe_2O_3††	1.63	1.72	1.43	2.11	2.70	3.53	3.65
FeO ††	14.1	14.9	12.4	18.2	23.5	30.3	31.4
MgO	15.3 (.4)	13.6 (.2)	16.9 (.2)	11.0 (.3)	7.55 (.3)	1.60 (.08)	1.55 (.08)
MnO	0.45 (.03)	0.48 (.03)	0.61 (.06)	0.16 (.02)	0.46 (.03)	0.75 (.05)	0.43 (.02)
TiO_2	1.47 (.16)	3.10 (.2)	2.12 (.2)	5.03 (.2)	3.97 (.3)	3.46 (.14)	3.11 (.3)
CaO	0.12 (.01)	0.05 (.01)	0.00 (.00)	0.06 (.01)	0.06 (.01)	0.46 (.10)	0.18 (.01)
Na_2O	0.07 (.01)	0.11 (.01)	0.14 (.02)	0.21 (.02)	0.09 (.01)	0.08 (.02)	0.06 (.01)
K_2O	9.77 (.2)	9.97 (.2)	10.0 (.1)	9.39 (.2)	9.39 (.1)	7.98 (.3)	8.28 (.3)
F	1.0 (.3)	1.0 (.3)	2.3 (.4)	0.3 (.1)	0.7 (.2)	0.4 (.4)	0.2 (.1)
Cl	0.08 (.02)	0.12 (.03)	0.10 (.01)	0.42 (.03)	0.44 (.08)	0.62 (.04)	0.52 (.09)
Total^	96.4	96.7	98.1	96.9	96.9	95.5	94.1
Si	5.76	5.68	5.97	5.74	5.74	5.78	5.79
Al	2.24	2.32	2.03	2.26	2.26	2.22	2.21
Σ (tet.)	8.00	8.00	8.00	8.00	8.00	8.00	8.00
Al	0.33	0.35	0.17	0.19	0.16	0.11	0.10
Fe^{+3}	0.19	0.20	0.16	0.25	0.33	0.47	0.48
Fe^{+2}	1.79	1.92	1.56	2.38	3.15	4.44	4.55
Ti	0.17	0.36	0.24	0.59	0.48	0.46	0.41
Mg	3.46	3.12	3.79	2.56	1.82	0.42	0.40
Mn	0.06	0.06	0.08	0.02	0.06	0.11	0.06
Σ (M_1-M_2)	6.00	6.01	6.00	5.99	6.00	6.01	6.00
K	1.89	1.96	1.92	1.87	1.94	1.78	1.83
Na	0.02	0.03	0.04	0.06	0.03	0.03	0.02
Ca	0.02	0.01	0.00	0.01	0.01	0.09	0.03
Σ (A)	1.93	2.00	1.96	1.94	1.98	1.90	1.88
F	0.48	0.48	1.09	0.15	0.36	0.22	0.11
Cl	0.02	0.03	0.03	0.11	0.12	0.18	0.15
F/Cl^^	24.0	16.0	36.3	1.4	3.0	1.2	0.73
F/F+OH	0.14	0.16	0.34	0.06	0.13	0.09	0.04
Fe/Fe+Mg	0.36	0.40	0.31	0.51	0.66	0.92	0.93
$X_{Phlogopite}$	0.58	0.52	0.63	0.47	0.30	0.07	0.07

*Number in parentheses is number of discrete biotite grains represented by average oxide values listed.

**Biotite is partly altered to chlorite.

***Value in parentheses is the greater of (a) the standard deviation for one of the individual analysis or (b) the spread between the average and the most extreme individual value.

†FeO value based on electron microprobe value for Fe.

$\Sigma[\text{tet.}+(M_1\text{-}M_2]=14$ for biotites from the Pliny Range, N.H.

Porphyritic Quartz Monzonite	Pink Biotite Granite		Granite Porphyry	Hastingsite Biotite Granite			Conway Granite	
85(2) ▲	94(2) △	114(1) ▽	34(2) ▲	166(4) ○	174(2) ◎	175(3) ●	82(1)** ◎	171_1(2) ◑
38.5 (.6)	38.1 (.4)	37.5 (.5)	35.4 (.6)	35.0 (.6)	35.5 (.5)	35.5 (.5)	34.6 (.5)	34.5 (.4)
12.8 (.2)	13.4 (.2)	12.4 (.1)	11.5 (.1)	12.1 (.3)	12.2 (.2)	11.7 (.2)	11.5 (.4)	11.9 (.2)
14.6 (.4)	16.3 (.2)	21.3 (.4)	30.0 (.5)	28.6 (.7)	28.1 (.3)	29.6 (.4)	32.4 (.6)	31.4 (.3)
1.53	1.71	2.25	3.15	3.00	1.66	3.11	3.40	4.75
13.2	14.8	19.3	27.2	25.9	26.61†††	26.8	29.3	27.15†††
15.6 (.3)	14.5 (.2)	10.2 (.2)	4.48 (.1)	4.96 (.5)	5.39 (.15)	4.97 (.2)	0.91 (.01)	3.24 (.13)
0.55 (.05)	0.42 (.03)	0.98 (.15)	0.77 (.13)	1.16 (.1)	0.95 (.02)	0.67 (.05)	0.33 (.03)	0.68 (.07)
2.88 (.17)	3.09 (.15)	3.35 (.35)	3.12 (.1)	3.55 (.6)	3.20 (.1)	3.50 (.1)	3.76 (.09)	3.44 (.1)
0.12 (.05)	0.02 (.01)	0.14 (.02)	0.07 (.01)	0.18 (.06)	0.11 (.01)	0.09 (.03)	0.14 (.02)	0.18 (.02)
0.08 (.01)	0.11 (.01)	0.07 (.01)	0.07 (.01)	0.07 (.01)	0.08 (.01)	0.09 (.01)	0.11 (.02)	0.05 (.01)
9.55 (.2)	9.78 (.2)	9.60 (.11)	8.97 (.12)	8.83 (.3)	9.15 (.1)	9.08 (.1)	7.44 (.15)	8.64 (.2)
1.3 (.3)	0.9 (.2)	1.5 (.3)	0.5 (.2)	0.9 (.4)	0.7 (.2)	0.9 (.3)	0.4 (.2)	0.5 (.3)
0.14 (.02)	0.15 (.02)	0.22 (.04)	0.32 (.03)	0.25 (.07)	0.35 (.07)	0.22 (.03)	0.22 (.03)	0.55 (.09)
96.5	97.0	97.3	95.6	95.9	95.9	96.4	92.1	95.6
5.88	5.81	5.91	5.92	5.82	5.87	5.88	6.08	5.83
2.12	2.19	2.09	2.08	2.18	2.13	2.12	1.92	2.17
8.00	8.00	8.00	8.00	8.00	8.00	8.00	8.00	8.00
0.18	0.22	0.23	0.19	0.19	0.25	0.16	0.46	0.20
0.18	0.20	0.27	0.40	0.38	0.21	0.39	0.45	0.60
1.69	1.89	2.56	3.80	3.60	3.68	3.71	4.31	3.84
0.33	0.35	0.40	0.39	0.44	0.40	0.41	0.50	0.44
3.55	3.29	2.41	1.12	1.23	1.35	1.23	0.24	0.82
0.07	0.05	0.13	0.11	0.16	0.13	0.09	0.05	0.10
6.00	6.00	6.00	6.01	6.00	6.00	5.99	6.01	6.00
1.86	1.90	1.94	1.91	1.87	1.93	1.92	1.67	1.86
0.02	0.03	0.02	0.02	0.02	0.03	0.03	0.04	0.02
0.02	0.00	0.02	0.01	0.03	0.02	0.02	0.03	0.03
1.90	1.93	1.98	1.94	1.92	1.97	1.97	1.74	1.91
0.63	0.43	0.75	0.26	0.47	0.37	0.47	0.22	0.26
0.04	0.04	0.06	0.09	0.07	0.10	0.06	0.07	0.16
15.8	10.8	12.5	2.9	6.7	3.7	7.8	3.1	1.6
0.20	0.14	0.28	0.10	0.18	0.13	0.17	0.10	0.11
0.35	0.39	0.54	0.79	0.76	0.75	0.77	0.95	0.84
0.59	0.55	0.40	0.19	0.20	0.22	0.20	0.04	0.14

††Ferrous iron calculated at 90.5 percent of total iron based on determination of 94.7 and 86.4 ferous iron in biotites 174 and 171, respectively.

†††Value determined by wet chemical methods.

Total is for partitioned Fe_2O_3, FeO values.

Atomic ratios.

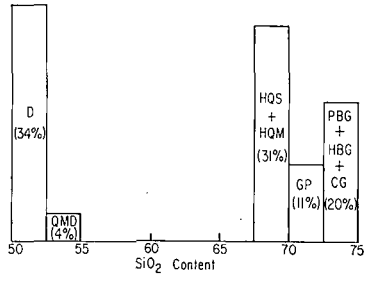

Fig. 4. Histogram showing percentage of outcrop area occupied by the younger WMMS units at the Pliny Range.

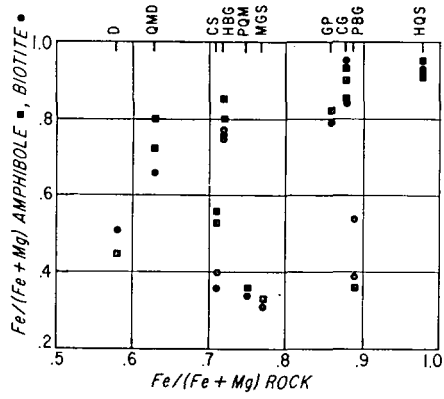

Fig. 5. Fe/(Fe+Mg) of amphiboles and biotites plotted against Fe/(Fe+Mg) of rocks of the Pliny Range.

Striking substitution mechanisms dominate the amphibole chemistry. Most common types of solid solution in amphiboles may be represented by the generalized formula,

$$(Na+K)_x Ca^{+2}_2(R^{+2}_{5-y-z}R^{+3}_y R^{+4}_z)(Al_{x+y+2z})(Si_{8-x-y-2z})O_{22}(OH)_2$$

Where Na^+ and K^+ occupy the otherwise vacant A-site; $R^{+2} = Mg^{+2}$, Fe^{+2}, Mn^{+2}; $R^{+3} = Al^{+3}$, Fe^{+3}; x = A-site occupancy; y = sum of Al^{VI} + Fe^{+3}; and $z = Ti^{+4}$.

Within the amphibole structure, in addition to simple substitutions such as Fe^{+2} for Mg, there are at least six possible schemes of coupled substitution which involve charge balancing and lead to idealized end members.

1.		*A* Na,K	+	TET. Al	for	*A* □	+	TET. Si	(Edenite)
2.	(a)	M_1-M_3 Al	+	TET. Al	for	M_1-M_3 Mg	+	TET. Si	(Tschermakite)
	or								
	(b)	Fe^{+3}	+	Al	for	Mg	+	Si	
3.	(a)	M_4 Na	+	M_1-M_3 Al	for	M_4 Ca	+	M_1-M_3 Mg	(Glaucophane)
	or								
	(b)	Na	+	Fe^{+3}	for	Ca	+	Mg	(Riebeckite)
4.		*A* Na	+	M_4 Na	for	*A* □	+	M_4 Ca	(Richterite)
5.		M_1-M_3 Ti	+	TET. 2Al	for	M_1-M_3 Mg	+	TET. 2Si	

		M_4		M_1-M_3		M_4		M_1-M_3
6.	(a)	2Na	+	Ti	for	2Ca	+	Mg
	or possibly							
	(b)	Na	+	Ti	for	Ca	+	Al

Calculated structural formulae (table 3) indicate that substitution mechanisms 1, 2(b), 3(b), and 6 are present in the amphiboles of the Pliny Range. With the exception of the coarse syenites, all Al is in tetrahedral coordination. The dominance of Al^{IV} in these amphiboles is compatible with the suggestion by Thompson (1947) that 4-coordinated Al is typical of minerals formed at high temperature and low pressure, whereas high pressure will favor Al^{VI}.

Fe^{VI} occupancy can vary by 100 percent with no necessary effect on content of $(Al+Fe^{+3})^{IV}$. (Two data sets are plotted in fig. 6B to demonstrate that plots for the summed 3-valent tetrahedral ions are tighter than those based on Al^{IV} alone in which all Fe is assumed to be Fe^{+2}.) These data are similar to the data from Finnmarka, where for Al^{IV} contents of about 1.0, total iron cations were either near 1.4 or 2.8 (Czamanske and Wones, 1973, fig. 2). Because a fixed percentage of total Fe is partitioned to Fe^{+3}, we cannot honestly check the relation of Al^{IV} content to the unit-cell occupancies of either individual iron species. However, a plot of $(Fe^{+3})^{VI}$ versus $(Al+Fe^{+3})^{IV}$ suggests that substitution 2(b) is present in the Pliny Range amphiboles. Additional substitution involving $(Al+Fe^{+3})^{IV}$ is also present, as shown in figure 6A in which A-site occupancy less Na^{M_4} is plotted against $(Al+Fe^{+3})^{IV}$.

Coupled substitution of type 1 is demonstrated by figure 6B in which total A-site occupancy is plotted against $(Al+Fe^{+3})^{IV}$. For comparison, two sets of data are plotted, one assuming all Fe as Fe^{+2}, the second, based on the one wet chemical determination, assuming that 69.5 percent of the total iron is ferrous. On the average, 2.5 tetrahedral sites are filled by 3-valent cations for each occupied A-site. This ratio is intermediate to the 1:1 ratio required by edenitic coupling (type 1) and a 4:1 ratio found by Robinson, Ross, and Jaffe (1971) for gedrites.

Plots of Na^{M_4} versus $(Al+Fe^{+3})^{VI}$ and A-site occupancy (figs. 7A and 7B) show that Na^{M_4} site occupancies are appreciably lower than required by strict type 3(b) and type 4 coupling, respectively. Weak correlations exist between related site occupancies for the primary Pliny Range amphiboles, but in those rocks that contain two generations of amphibole, trends exist that are distinctly opposed to coupled substitution of types 3(b) and 4. In contrast, the compensation of Na^{M_4} by Ti^{+4} in octrahedral coordination, that is substitutions 6(a) and 6(b), is clearly demonstrated in figure 7C. Not only do the majority of the amphiboles contain Na^{M_4} and Ti^{+4} in the correct proportions to satisfy substitutions 6(a) and 6(b), but also the trends shown by two generations of amphibole within single units are of this type. The Pliny Range amphiboles are believed to be the first group of amphiboles for which type 6 coupling is demonstrable. At Finnmarka, where somewhat less sodic and iron-rich amphiboles are

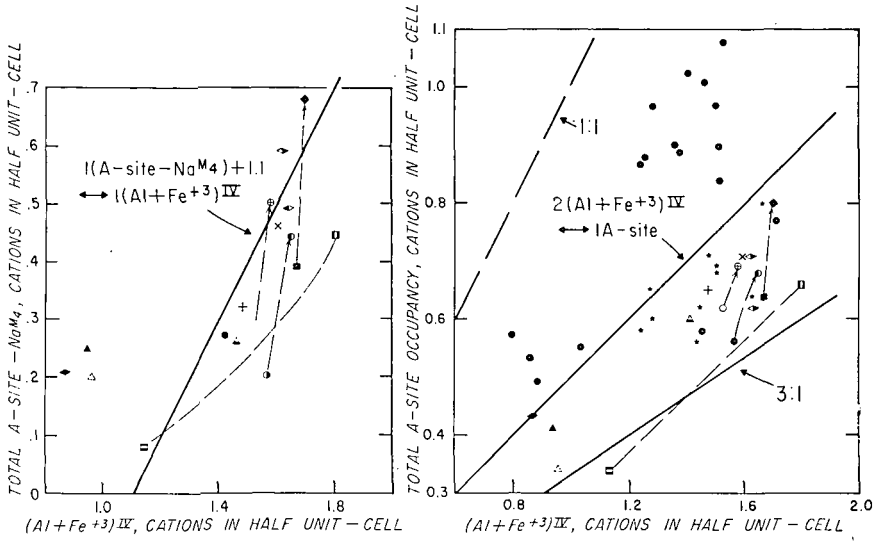

Fig. 6A. Plot of total A-site cations less Na^+ in the M_4 site versus $(Al+Fe^{+3})^{IV}$ for amphiboles of the Pliny Range. For identity of the symbols used in figures 6 through 12, see the headings of tables 3 and 4. On this and other figures a secondary amphibole lies at the head of the arrow connecting it with the primary amphibole. The two amphiboles in W do not appear to share the same replacement relation and are connected by a dashed line.

B. Plot of total A-site cations versus $(Al+Fe^{+3})^{IV}$ for amphiboles of the Pliny Range. Smaller dots in upper portion of figure are for total Fe = FeO. Stars directly to the left of some symbols show location of symbol if $(Fe^{+3})^{IV}$ is subtracted.

present, Ti^{+4} was not coupled to Na^{M_4} but was involved in coupling with Al^{IV} (type 5). A unit-cell occupancy plot of Ti^{+4} against $(Al+Fe^{+3})^{IV}$ for the Pliny Range amphiboles shows that unit-cell content of Ti^{+4} varies from 0.04 to 0.33 Ti^{+4} at 1.5 $(Al+Fe^{+3})^{IV}$.

Substitutions of Na^+ or K^+ in the A-site and R^{+3} or Ti^{+4} in the octahedral site, compensated by substitution of Al for Si in the tetrahedral sites, should result in $(Al+Fe^{+3})^{IV}$ = A-site occupancy + $[(R^{+3})^{VI}+2Ti^{+4}]$ (Robinson, Ross, and Jaffe, 1971). This condition is not satisfied (fig. 7D). The imbalance shown by figure 7D is attributed predominantly to excess charge associated with Ti^{+4} (type 6 coupling). As shown in figure 7D, subtraction of the adjusted Ti^{+4} site occupancy ($2Ti^{+4}$) leaves a residual which indicates an irregular component of riebeckitic substitution (type 3(b)) in the Pliny Range amphiboles.

The presence of tetrahedral Fe^{+3} in the Pliny Range amphiboles is suggested by the data of table 3 and supported by calculations in which Fe^{+3}/Fe^{+2} is arbitrarily varied. Calculations that assume that all Fe is ferrous yield tetrahedral $(Si^{+4}+Al^{+3})$ barely exceeding 8.00, with A-site occupancies between 0.50 and 1.08; 12 of 16 are above 0.77, and 3 above 1.00. Robinson, Ross, and Jaffe (1971) consider 0.60 a typical upper limit to A-site occupancy, although 1.00 is possible for ideal end mem-

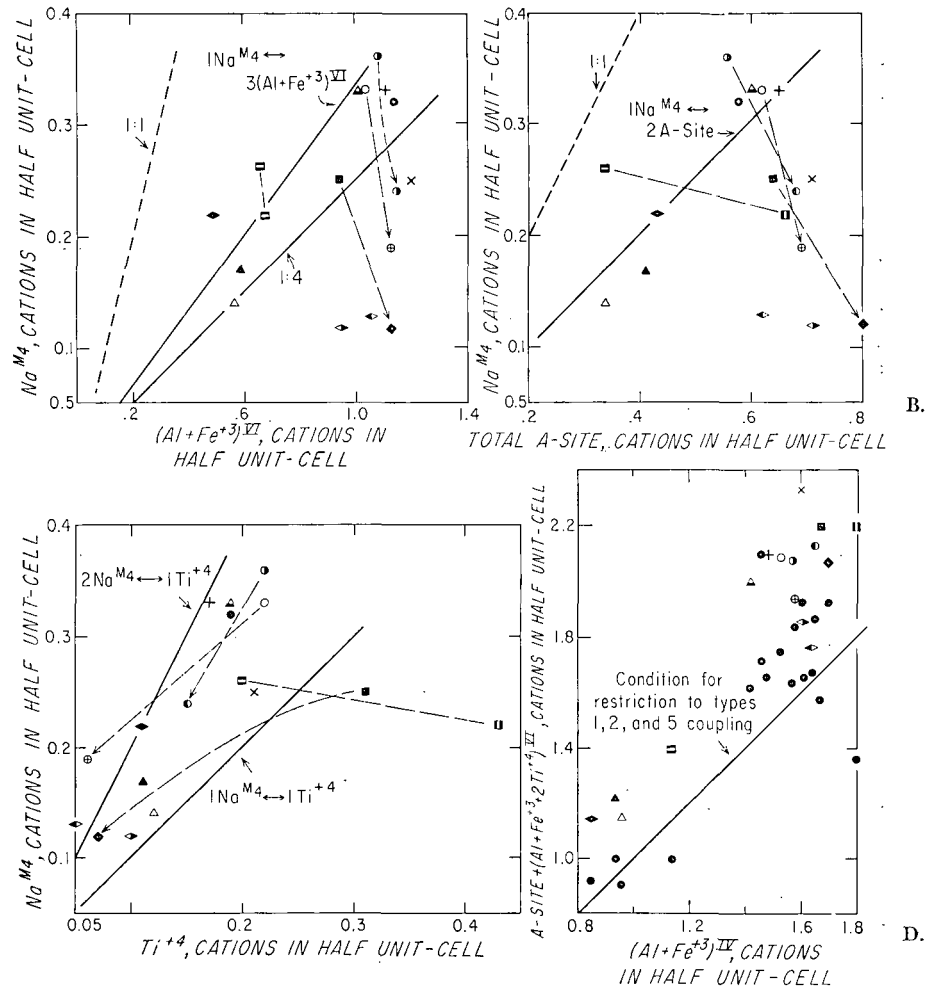

Fig. 7A. Na^{+} in the M_4 site versus $(Al+Fe^{+3})^{IV}$ for amphiboles of the Pliny Range. Symbols as for figure 6.

B. Na^{+} in the M_4 site versus total A-site occupancy for amphiboles of the Pliny Range.

C. Na^{+} in the M_4 site versus total Ti^{+4} for amphiboles of the Pliny Range.

D. A-site cations plus $(Al+Fe^{+3}+Ti^{+4})^{VI}$ versus $(Al+Fe^{+3})^{IV}$ for amphiboles of the Pliny Range. Solid dots in lower portions of figure represent A-site + $(Al+Fe^{+3})^{VI}$.

TABLE 5
Electron microprobe analyses and unit-cell occupancies for pyroxenes and chlorites from the Pliny Range, N.H.

Specimen Number	Pyroxenes		Chlorites				
	W_1(1)	W_2(1)	178 (1)	W (1)	114 (2)	174 (2)	175 (1)
SiO_2	51.0 (.06)	46.9 (.16)	29.5 (.3)	26.1 (.3)	26.9 (.5)	23.6 (.3)	23.2 (.7)
Al_2O_3	2.68 (.02)	6.02 (.09)	16.9 (.2)	18.0 (.5)	17.7 (.6)	18.6 (.5)	18.2 (.3)
FeO*	9.87 (.8)	9.86 (.9)	18.7 (.2)	27.4 (.5)	24.0 (.4)	34.9 (.3)	39.7 (.7)
MgO	12.8 (.8)	12.5 (.7)	20.3 (.4)	13.9 (.5)	16.8 (.4)	7.40 (.3)	3.00 (.09)
MnO	0.40 (.02)	0.36 (.1)	0.86 (.03)	0.19 (.01)	0.60 (.07)	1.02 (.14)	0.73 (.02)
TiO_2	1.03 (.1)	3.00 (.1)	0.00	0.00	0.00	0.00	0.19 (.09)
CaO	20.8 (.3)	20.6 (.6)	0.05 (.01)	0.06 (.01)	0.06 (.01)	0.07 (.01)	0.15 (.01)
Na_2O	0.64 (.09)	0.77 (.09)	0.00	0.01 (.01)	0.02 (.01)	0.03 (.01)	0.03 (.01)
K_2O	0.04 (.01)	0.00	0.00	0.05 (.01)	0.00	0.01 (.01)	0.25 (.13)
Total	99.26	100.01	86.31	85.71	86.08	85.63	85.45
Si	1.93	1.77	6.09	5.71	5.76	5.45	5.53
Al	0.07	0.23	1.91	2.29	2.24	2.55	2.47
Σ (tet.)	2.00	2.00	8.00	8.00	8.00	8.00	8.00
Al	0.05	0.04	2.21	2.36	2.22	2.51	2.64
Fe	0.31	0.31	3.23	5.02	4.30	6.74	7.91
Mg	0.72	0.70	6.25	4.53	5.36	2.55	1.07
Mn	0.01	0.01	0.15	0.04	0.11	0.20	0.15
Ti	0.03	0.09	0.00	0.00	0.00	0.00	0.03
Ca	0.84	0.83	0.01	0.01	0.01	0.02	0.04
Na	0.05	0.06	0.00	0.00	0.01	0.01	0.01
K	0.00	0.00	0.00	0.01	0.00	0.00	0.08
Σ	2.01	2.04	11.85	11.97	12.01	12.03	11.93
Fe/(Fe+Mg)	0.31	0.31	0.34	0.53	0.44	0.73	0.88

*All Fe calculated as FeO.

TABLE 6
Partial electron microprobe analyses of allanites from the Pliny Range, N.H.

Rock Name	Pink Biotite Granite	Granite Porphyry	Hastingsite Biotite Granite					Conway Granite		
Specimen Number	94	34	166,1*	166,2	174,1	174,2	174,3**	82,1	82,2	28***
SiO_2	27.5	27.3	25.9	24.3	27.2	27.1	24.7	23.7	22.8	26.05
Al_2O_3	13.8	8.35	11.4	11.1	10.7	11.2	11.6	9.11	9.38	7.54
FeO†	15.3	25.7	19.6	18.1	20.8	20.3	18.0	20.8	21.3	n.d.
MgO	1.30	0.30	0.43	0.43	0.62	0.45	0.39	0.20	0.16	0.81
MnO	0.67	0.62	0.70	0.72	0.53	0.59	0.64	0.40	0.41	0.58
TiO_2	2.89	4.29	4.05	3.89	3.59	3.16	3.12	5.29	5.26	n.d.
CaO	8.78	5.71	6.75	6.47	7.52	8.42	6.77	6.55	5.95	10.45
Na_2O	0.20	0.20	0.31	0.36	0.25	0.27	0.35	0.24	0.30	n.d.
K_2O	0.15	0.09	0.14	0.17	0.10	0.10	0.13	0.09	0.11	n.d.
Total	70.59	72.56	69.28	65.54	71.31	71.59	65.70	66.38	65.67	

* 166,1 refers to allanite grain 1 in specimen 166.
** Analysis 174,3 represents a later overgrowth on 174,2.
*** Analysis 28, table 17 of Billings and Wilson (1964). Also: Fe_2O_3 — 17.01; H_2O — 5.60; Ce_2O_3 — 12.45; other R.E.'s — 18.69.
† Total iron calcaulated as FeO.

TABLE 7

Electron microprobe analyses for magnetites and ilmenites

	Coarse Syenite	Medium-grained Syenite		Diorite		
	178	138		W		
	Mt	Mt	Ilm	Mt_1	Mt_2	Ilm
Weight Percent**						
FeO	97.1 ±.4***	91.1 ±.4	25.4±1.0	82.1 ±.3	92.0 ±.4	47.9 ±.1
TiO_2	0.47±.05	0.71±.1	49.9±1.0	9.75±.5	0.40±.04	48.2 ±.2
MnO	0.16±.02.	0.22±.02	23.0±1.0	0.56±.04	0.20±.02	2.06±.04
Molecular Percent†						
Fe_2TiO_4; $FeTiO_3$	1.04	1.72	46.17	28.14	0.84	88.44
Fe_3O_4; Fe_2O_3	98.74	97.92	4.08	70.92	98.83	7.14
Mn_2TiO_4; $MnTiO_3$	0.22	0.36	49.75	0.94	0.32	4.43
$100 \times \frac{Fe_2TiO_4}{Fe_2TiO_4+Fe_3O_4}$	1.10	1.73	--	28.41	0.84	--
$100 \times \frac{Fe_2O_3}{Fe_2O_3+FeTiO_3}$	--	--	8.12	--	--	7.47
K_D††		0.007		0.291	0.128	

	Granite Porphyry		Pink Biotite Granite			
	34		94		114	
	Mt	Ilm	Mt	Ilm	Mt	Ilm
Weight Percent**						
FeO	89.8 ±.2	41.9±1.6	91.2 ±.4	48.4±1.0	91.6 ±.4	40.0±1.0
TiO_2	2.9 ±.2	48.6± .5	0.30±.1	44.1±1.0	0.54±.1	50.4± .4
MnO	0.43±.07	7.5±1.2	0.18±.02	3.6± .1	0.09±.01	8.3±1.
Molecular Percent†						
Fe_2TiO_4; $FeTiO_3$	7.72	77.41	0.59	78.54	1.43	78.71
Fe_3O_4; Fe_2O_3	91.57	6.23	99.12	13.51	98.42	3.30
Mn_2TiO_4; $MnTiO_3$	0.70	16.36	0.30	7.95	0.15	17.99
$100 \times \frac{Fe_2TiO_4}{Fe_2TiO_4+Fe_3O_4}$	7.78	--	5.86	--	1.43	--
$100 \times \frac{Fe_2O_3}{Fe_2O_3+FeTiO_3}$	--	7.45	--	14.68	--	4.02
K_D††	0.62		0.059		0.013	

* Two relatively distinct compositions present.

** MgO < 0.05 for all analyses.

*** ± values shown only to give some indication of homogeneity as disclosed in this reconnaissance.

bers. The formulae of table 3 assume that 69.5 percent of the iron is Fe^{+2} (based on amphibole 178), result in A-site occupancies between 0.34 and 0.80, and require that Fe^{+3IV} is present in 9 of 16 samples. Calculations for analysis 171_2 were made at 5 percent increments of Fe^{+2} content. Fe^{+3IV} is required as the Fe^{+2} percentage drops from 90 to 85, with the corresponding A-site occupancy between 0.86 and 0.79 ions. Borley and Frost (1963) and Gorbatschev (1969) also present amphibole analyses that suggest the presence of Fe^{+3IV}. Hazen and Wones (1972) demonstrated that, in Al-deficient systems, Fe^{+3IV} is found in biotites and, by analogy, amphiboles.

As seen on most plots, the compositions of the two amphiboles in the diorite are related in a manner quite different from the way in which the primary and secondary amphiboles are related in samples 46, 166,

from the Pliny Range, N.H.

Quartz Monzodiorite		Hastingsite Quartz Syenite					Porphyritic Quartz Monzonite	
46		163		164			85	
Mt	Ilm	Mt	Ilm	Mt *	Mt	Ilm	Mt	Ilm
92.3 ±.4	44.2 ±1.0	89.5 ±.3	41.0±1.0	79.7 ±.4	88.4 ±.4	47.2±1.0	92.0 ±.4	31.0±1.0
0.77±.1	50.3 ± .2	1.61±.14	48.7± .2	10.2 ±.3	2.5 ±.4	48.7± .4	0.37±.05	51.3±1.0
0.23±.02	5.23± .3	0.24±.02	7.4± .8	0.96±.05	0.30±.04	2.8±1.4	0.11±.01	16.9±1.0
1.85	84.22	4.36	78.64	29.00	6.91	87.23	0.90	61.67
97.77	4.59	95.24	5.08	69.37	92.59	6.73	98.92	2.11
0.38	11.18	0.40	16.28	1.62	0.50	6.05	0.18	36.23
1.86	--	4.38	--	29.48	6.94	--	0.90	--
--	5.17	--	6.07	--	--	7.16	--	3.31
0.122		0.13		0.366	0.136		0.005	

Hastingsite Biotite Granite						Conway Granite			
166		174		175		82		171	
Mt	Ilm	Mt	Ilm	Mt	Ilm	Mt	Ilm	Mt	Ilm
92.3 ±.4	35.7±0.9	93.0 ±.5	41.4±.4	91.7 ±.5	44.8 ±.4	86.9 ±.5	47.6±.2	90.5 ±.5	44.1±.1
0.77±.1	48.1± .1	0.66±.02	50.0±.5	0.54±.02	48.7 ±.4	5.4 ±.3	48.5±.5	0.83±.05	48.7±.3
0.23±.02	13.6±1.0	0.15±.02	8.6±.4	-0.10±.02	4.6 ±.3	0.55±.05	2.0±.1	0.15±.02	4.8±.1
1.84	63.71	1.66	76.23	1.41	83.79	14.88	89.39	2.20	84.01
97.78	6.67	98.10	5.46	98.42	6.10	84.22	6.36	92.55	5.59
0.37	29.62	0.24	18.32	0.17	10.10	0.91	4.25	0.25	10.40
1.85	--	1.66	--	1.42	--	15.01	--	2.21	--
--	9.48	--	6.68	--	6.79	--	6.64	--	6.24
0.016		0.020		0.027		0.336		0.066	

† Calculations according to Anderson (1968).

††$K_D = (FeO_{Ilm} + MnO_{Sp})/(FeO_{Sp} + MnO_{Ilm})$; value for pair entered under magnetite analysis.

and 171. The distinction between the two amphiboles in W (figs. 6 and 7) is primarily a result of the large difference in their Al^{IV} content and the coupled variation in A-site occupancy; the substantial difference in Ti^{+4} content seems less significant. Textures observed in thin section and the chemical data of tables 3 and 5 suggest that the amphibole W_1 is a replacement of pyroxene, whereas amphibole W_2 is primary. The chemical influence of the preexisting pyroxene in the diorite contrasts with the presumed late formation of blue-green amphibole in 46, 166, and 171.

A perspective on the Pliny Range amphiboles is possible through consideration of amphibole analyses from other units of the WMMS and from comparable geologic settings. Prior to our study, the only amphibole analyses for WMMS rocks known to us were those in Billings and Wilson (1964); see table 7, analyses 8-13). The low-Al hastingsites and ferro-

hastingsites found by Creasy (1974) and ourselves have not been well known in New England. However, amphiboles similar to those of the Pliny Range are typical of other classic areas of high-level granitic intrusions and ring complexes, which are further characterized by alkali amphiboles and rocks of peralkaline or near peralkaline composition (Borley and Frost, 1963; Borley, 1963; Simonen and Vorma, 1969; Barker and others, 1975; Czamanske and Wones, 1973).

The known Pliny Range amphiboles, many amphiboles from the classic alkaline granite areas, and the amphiboles studied by Billings (1928) and Buddington and Leonard (1953) are calcic amphiboles with CaO contents in the range 9.5 to 11.5 wt percent and unit-cell Ca contents of 1.50 (see Leake, 1968). The Al_2O_3 content of these calcic amphiboles ranges from 4 to 12 wt percent or from less than 0.7 to 2.2 Al cations per unit-cell. The Pliny Range amphiboles cover 70 percent of this range with the high-Al amphiboles in the older syenites and the diorite, as might be expected. Na_2O contents for these calcic amphiboles range from 1.2 to almost 3 wt percent, with most values less than 2.3.

To our knowledge no alkali amphiboles have developed in the Pliny Range, in contrast to other regions of White Mountain plutonism and Nigeria. Typical characteristics of these alkali amphiboles, in addition to high Na_2O content, are significantly lower concentrations of CaO and Al_2O_3. The lack of alkali amphiboles in the Pliny Range is in keeping with the lack of peralkaline normative components (table 2).

Amphiboles from high-level granitic intrusions are characterized by appreciable contents of F and Cl. Fluorine and chlorine contents for Pliny Range amphiboles and biotites are given in tables 3 and 4. Aside from the two mafic units, high Cl contents are typical of the more evolved rock units, and, conversely, high F/Cl ratios are typical of amphiboles and biotites with low Fe/(Fe+Mg). These results agree well with the experimental data of Munoz and Ludington (1974). $F_{Amp}/F_{Bio}>1$ (table 8) is another distinction of the hastingsite quartz syenite, granite porphyry, and Conway granite, three units that have high Fe/(Fe+Mg) and may represent the products of extended fractional crystallization or zone refining. The secondary blue-green amphiboles in samples 46, 166, and 171 are substantially enriched in Cl, while Na_2O content is diminished. The extreme changes in F/Cl for the secondary amphiboles must reflect both changing temperature and changes in the regime of the crystallizing amphibole and imply that Cl was preferentially concentrated in the post-magmatic fluids.

Borley (1963) and Borley and Frost (1963) have focused on the fact that the Nigerian and southern Rhodesian alkali amphiboles and ferrohastingsites contain Zn. Zn has also been found in alkali amphibole from the Percy quadrangle (Billings and Wilson, 1964). Zn contents obtained for selected Pliny Range amphiboles and biotites are briefly summarized as follows (where A and B stand for amphibole and biotite respectively): 155-B, 138-A, 138-B, W-A, 94-A, and 94-B, 0.00; 155-A and

W-B, 0.04; 163-A, 0.07; 171-A, 0.10; 171-B, 0.16; and 163-B, 0.19 wt percent ZnO. Zn is enriched in mafic silicates with high Fe/(Fe+Mg) and in biotite relative to amphibole.

Biotites

Biotite is present in all map units in concentrations ranging from a trace to over 10 percent (table 1). The biotites of the Pliny Range were analyzed by electron microprobe with two samples, 174 and 171, analyzed for Fe_2O_3 content as well. We lack analyses for Rb, Li, and H_2O, all of which can be present in significant amounts (Neiva, 1976).

In this study we exploit the mole fractions of Fe^{+2}, Mg^{+2}, and F^- which are dependent on the calculation scheme, as well as ratios such as (K+Na)/Al and Fe/(Fe+Mg) which are not. As noted, we will have maximum estimates of $X_{Mg^{+2}}$ and $X_{Fe^{+2}}$ in all the discussions involving the derivation of intensive parameters from biotite phase equilibria.

Fosters' (1960) study of the trioctahedral micas is a valuable point of reference. The biotites from the Pliny Range are notably low in

TABLE 8

K_D values representing the co-distribution of Mn, Ti, Cl, and F between amphiboles and biotites of the Pliny Range, N.H.

Rock Type	Sample Number	K_D (Mn_{Amp}/Mn_{Bio})	K_D (Ti_{Amp}/Ti_{Bio})	K_D (Cl_{Amp}/Cl_{Bio})	K_D (F_{Amp}/F_{Bio})
Coarse Syenite	155	1.36	0.29	0.87	1.00
Medium-grained Syenite	138	1.48	0.46	1.00	0.52
Diorite	W_1	2.56	0.36	0.24	1.00
	W_2	1.94	0.77		
Quartz	46_1	1.80	0.68	0.55	0.68
Monzodiorite	46_2	1.57	0.15		
Hastingsite	163	1.48	0.49	0.76	1.80
Quartz Syenite	164	1.73	0.44	0.75	5.01
Porphyritic Quartz Monzonite	85	2.00	0.34	0.72	0.46
Pink Biotite Granite	94	1.48	0.35	0.74	0.45
Granite Porphyry	34	2.10	0.50	1.07	2.00
Hastingsite	166_1	1.47	0.52	1.00	0.78
Biotite Granite	166_2	1.59	0.14		
Conway Granite	82	2.61	0.43	1.77	1.50
	171_1	1.96	0.51	0.67	1.20
	171_2	1.91	0.36		

aluminum but are not atypical for rocks of this type. Foster's group of low-Al biotites ranges from 11 to 16.3 wt percent Al_2O_3 and averages 14.6; for the Pliny Range the average is only 12.4, the range 11.3 to 14.7 wt percent. In comparison, four analyses of biotite from the White Mountain batholith average 13.2 wt percent Al_2O_3 (Creasy, 1974), four from the rapakivi of Finland average 11.9 (Simonen and Vorma, 1969), four from the Pikes Peak batholith average 12.2 (Barker and others, 1975), and nine from Finnmarka average 11.8 (Czamanske and Wones, 1973). Another distinction the Pliny Range biotites share with biotites from the aforementioned areas is an excess of Al over K+Na in the unit cell. For the Pliny Range biotites (K+Na)/Al averages 0.81, ranges from 0.74 to 0.89, and shows no systematic variation with Fe/(Fe+Mg) (aberrant analysis 82 has not been included).

Calculations of cation distribution within the octahedral layer of the Pliny Range biotites show that $(Fe^{+2}+Mn^{+2})/(Fe^{+2}+Mn^{+2}+Mg^{+2})$ of these biotites ranges from 0.32 to 0.95. The biotites have a very small number of R^{+3} and R^{+4} cations and are on the lower limit of $(Fe^{+2}+Mn^{+2})$ content defined by Foster (1960). Their position within this limit supports the findings of Hazen and Wones (1972) that Fe^{+2} and Mn^{+2} mica end members are inherently unstable.

We have already noted that despite a substantial range in Fe/(Fe+Mg) there are certain notable similarities in biotite unit-cell occupancies and charge compensation. Further consideration of table 4 shows that there are no regular or substantial differences in unit-cell content of Al^{IV}, Ti, or Mn, three variables that might have been expected to show some correlation with Fe/(Fe+Mg), rock type, or mineral assemblage. A significant factor that may partly account for this surprising uniformity in biotite composition is that biotite always coexists with amphibole and alkali feldspar in the Pliny Range rocks. A suite of rocks containing biotites of similarly diverse Fe/(Fe+Mg) would commonly contain mafic mineral associations that evolved from biotite + pyroxene → biotite + amphibole → biotite alone (for example Nockolds, 1947).

Three analyses of table 4 merit brief mention. The low K_2O content and implication of extra water in the low sum for biotite from sample 82 suggest alteration to chlorite, as do the facts that the composite layer charge is only −1.73 (Foster, 1960), and the phase is depleted in Mg. The low modal abundance (table 1), low K_2O, and the low sums suggest that the biotite from the hastingsite quartz syenite (163 and 164) may have become unstable as crystallization ceased.

Chlorites

Small amounts of chlorite are present in a number of the rock units of the Pliny Range (see app), and over 7 percent chlorite is present in diorite specimen W. Most of the observed chlorite appears to have formed in a post-magmatic environment as a replacement of biotite. While it is thus not surprising that Fe/(Fe+Mg) for chlorite and biotite are similar for a given sample (compare tables 4 and 5), rock suites are known in

which replacement chlorite contains more or less total Fe relative to Mg than coexisting biotite. Analyses presented in table 5 represent averages over numerous grains in localized patches of chlorite. Chlorite compositions are quite ordinary and, with the exception of analysis 175, show the customary quantitative removal of TiO_2, K_2O, and Na_2O with respect to their biotite precursors.

Pyroxenes

In samples chosen for the present study, substantial clinopyroxene (salite) occurs only in the diorite, W, although minor relict pyroxene also occurs in the quartz monzodiorite (tables 1 and 5). Deer, Howie, and Zussman (1963) note that salites are not common in plutonic rocks but are "particularly characteristic in hypabyssal rocks derived from alkali basalt magmas."

Two distinct pyroxene populations are present in the diorite. The marked difference in TiO_2 content indicates that variation in Si:Al is not the sole factor involved. The pyroxene with higher TiO_2 content (W_2, table 5), has a distinct pinkish cast and occurs as somewhat larger grains than the variety with lower TiO_2 content. Crystallization of late, intersertal sphene could have lowered the activity of TiO_2 and caused the observed changes in the pyroxene composition.

Allanites

Allanite is a common accessory in silicic WMMS units and in similar rocks throughout the world. Partial analyses of a number of Pliny Range allanites are presented in table 6. The analyses are rather unlike the cited analysis reported by Billings and Wilson (1964, table 17) for allanite from the Conway granite at Conway. The Pliny Range allanites contain more iron, markedly more titanium, and apparently more rare earth elements (R.E.E.) than are typical of the allanite analyses compiled by Deer, Howie, and Zussman (1962). The low sums of table 6 relate to the fact that allanites contain 1 to 3 percent H_2O^+ and substantial amounts of R.E.E.

Allanite iron contents faithfully reflect the changes in chemical environment shown by the amphiboles and biotites, as shown dramatically in the comparison of samples 94 and 34, but also by consideration of the remaining analyses. The notable correlations between Al_2O_3, total iron, and CaO contents are in accord with substitutional schemes as reviewed by Deer, Howie, and Zussman. Because the reported analyses are incomplete and lack determination of Fe^{+3}/Fe^{+2}, these schemes cannot be explored in detail.

Opaque oxides

Despite the fact that study of opaque oxides in similar plutonic rocks had proven difficult to interpret (Czamanske and Mihálik, 1972), a microprobe reconnaissance was made of the oxide phases in the Pliny Range rocks (table 7). In specimens 138, 164, 85, 34, and 94 ilmenite is a scarce phase. Coarse syenite specimen 178 contains coarse sphene but no il-

menite, and in medium-grained syenite specimen 138, ilmenite is present as rare cores in large sphene. The suggested replacement of ilmenite by sphene in some of the Pliny Range rocks may be a result of late magmatic oxidation (Czamanske and Mihálik, 1972). In accord with this theory, 138 also contains large, angular, primary hematite. Specimen 164 contains abundant ilmenite and only scarce, inhomogeneous magnetite.

The ilmenites contain appreciable and sometimes varying amounts of manganese, and the magnetites often bear variable amounts of titanium. In all but five instances, the TiO_2 content of the magnetites is below 1.0 wt percent. Measured variations in TiO_2 content are taken to reflect variations in the conditions and rock volumes with which the magnetites were in equilibrium. The compositions of magnetites in specimens W, 164, and 82 may relate to conditions of crystallization. The total magmatic history of the opaque oxides in samples W, 164, and 82 cannot have been very dissimilar, despite the fact that these rocks are widely divergent in composition and separated in the intrusive sequence.

The compositions of ilmenites in the Pliny Range rocks range from 46.2 mole percent $FeTiO_3$, for ilmenite that coexists with hematite in the medium-grained syenite (138), to 89.4 mole percent $FeTiO_3$, for ilmenite from the Conway granite (82). Manganese contents of the Pliny Range ilmenites are appreciable; except for the diorite, at least one specimen in each unit contains over 10 mole percent $MnTiO_3$. Although late magmatic oxidation reactions may have destroyed ilmenite in the Pliny Range rocks, $MnTiO_3$ contents in the Pliny Range ilmenites are not simply a function of FeO activity, in contrast to the assemblages at Finnmarka (Czamanske and Mihálik, 1972). There is no correlation between mole percentage of $MnTiO_3$ in ilmenite and: (1) mole percent Fe_2O_3 in ilmenite, (2) whole-rock Fe^{+3}/Fe^{+2}, (3) whole-rock Fe/(Fe+Mg), or (4) biotite Fe/(Fe+Mg).

The key to understanding the Mn contents of the ilmenites lies in figure 8, in which the mole fraction of $MnTiO_3$ in ilmenite is related to the atomic fraction of Mn in the M_1-M_2 sites of the coexisting biotite. With the exception of the two most oxidized rocks, containing biotite with the lowest FeO contents, there is a striking correlation between these variables. Because the sparse ilmenite in specimen 94 of the pink biotite granite contains a modest amount of $MnTiO_3$ and the abundant ilmenite in specimen 114 contains twice as much, it does not seem reasonable to suggest, as Czamanske and Mihálik (1972) did for the Finnmarka Complex, that Mn enrichment in ilmenite is caused by residual concentration in a diminished amount of ilmenite. Similarly, among hastingsite biotite granite specimens 166, 174, and 175, the sample with the least opaque oxides (175, table 1) also shows the least Mn-enrichment. It simply appears that, with two exceptions, there has been preserved a remarkably consistent partitioning of Mn between ilmenite and biotite and that the absolute amounts of Mn in these two phases relate to the availability of Mn as they crystallized. Biotite does not readily

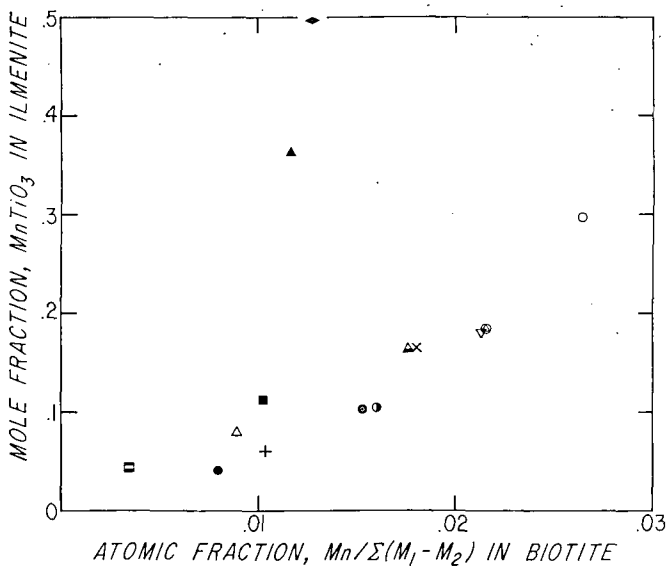

Fig. 8. Plot of mole fraction $MnTiO_3$ in ilmenite against atomic fraction Mn^{+2} in coexisting biotite for rocks of the Pliny Range.

accept Mn into its structure because of a significant difference in the size of the octahedral Mg^{+2}, Fe^{+2}, and Mn^{+2} cations (Hazen and Wones, 1972). MnO will be preferentially partitioned into ilmenite, and the partitioning should be greater for MgO-rich biotites. The two most Mn-rich ilmenites are in rocks (138 and 85) that are clearly among the most oxidized as judged from biotite Fe/(Fe+Mg) and whole rock Fe^{+3}/Fe^{+2}.

We feel that the regular Mn-partitioning between biotite and ilmenite and the substantial TiO_2 contents of the biotites indicate that these two phases equilibrated under magmatic conditions. On the other hand, generally low and variable TiO_2 contents suggest that the magnetites represent equilibration at lower temperatures, either by recrystallization or by formation during post-magmatic oxidation. The distribution coefficient or Mn between spinel and ilmenite $K_D = FeO^{Ilm} \times MnO^{Mt}/FeO^{Mt} \times MnO^{Ilm}$ was shown by Mazullo, Dixon, and Lindsley (1975) to be between 0.420 at 700°C and 0.580 at 850°. Values of K_D for the Pliny Range samples are above 0.29 for only the diorite, hastingsite quartz syenite, and Conway granite, the only samples for which the Buddington and Lindsley geothermometer yields magmatic temperatures.

The high Fe_2O_3 content of the ilmenite from pink biotite granite specimen 94 neatly corroborates the distinct indication of oxidation provided by the mafic silicate data (tables 3 and 4). The environment in which specimen 94 crystallized was distinct from that recorded in specimen 114 from the opposite end of the ring dike (see fig. 1). As noted earlier, that part of the dike from which specimens 114 and 115 were

collected is the only area in which pink biotite granite matrix predominates over inclusions.

MAFIC SILICATE INTERRELATIONS

Recognition of equilibrium and disequilibrium mineral assemblages based on examination of elemental partitioning has been the subject of numerous scientific contributions. The present study provides important data bearing on proposed indices of equilibria between coexisting amphibole and biotite because: (1) four of the units contain two discrete amphiboles, (2) the rocks of the Pliny Range form a coherent suite, and (3) the syenites are clearly older than the remaining units and have possibly recrystallized.

Gorbatschev (1969 and 1970) has stressed the utility of several means for establishing chemical equilibrium between amphibole and biotite. On the basis of the Pliny Range data, we question the utility of several of his methods and suggest that microscopic observations, combined with casual inspection of the data in tables 3 and 4, would be nearly as informative. Following Gorbatschev (1970), we plotted the mole fractions of Al^{IV} in biotite ($X^{Bio}Al^{IV}$) and amphibole ($X^{Amp}Al^{IV}$) against one another. Our data do not follow the relation proposed by Gorbatschev, and we suggest that he erred in proposing a single equation for all intrusive sequences. More disturbing is the fact that in the three cases where two amphiboles are present in a replacement relationship, there is virtually no indication of disequilibrated amphibole and biotite despite the fact that significant changes in unit-cell occupancy of Ti^{+4} and Na have taken place (fig. 7C). This and previous arguments counter Gorbatschev's (1970) premise that "the electro-neutrality of amphibole appears to rely primarily on tetrahedral substitutions."

A second type of plot utilizing Fe/(Fe+Mg) is often made (for example, Gorbatschev, 1969; and Leake, 1968) to examine the relation between amphiboles and biotites. We believe it is preferable on crystal chemical grounds to plot $Fe/\Sigma(M_1\text{-}M_2)$ for biotite versus $Fe/\Sigma(M_1\text{-}M_3)$ for amphibole. On this basis, the Pliny Range analyses are plotted in figure 9 where they fall near a slope of 1.0. The most deviant point represents coarse syenite sample 155, noted earlier to contain conspicuously fresh amphibole which we suspect has recrystallized. Amphiboles in the coarse syenite are the most aluminous in the Pliny Range. Because increased Al content enhances the stability of amphibole for a given Fe-content the exchange with biotite is shifted to favor Fe in the amphibole. The secondary amphiboles in samples 46, 166, and 171 are also enriched in Fe relative to biotite. There is thus good evidence that: (1) Fe and Cl enrichment continued in the residual fluids from which crystallization took place; (2) secondary amphiboles reflect these changes; and (3) in general our data reflect primary partitioning between amphibole and biotite.

Gorbatschev's arguments that there should be a relation between Fe/(Fe+Mg) and both Al^{IV} codistribution and the sum of Al^{VI} and Ti^{VI}

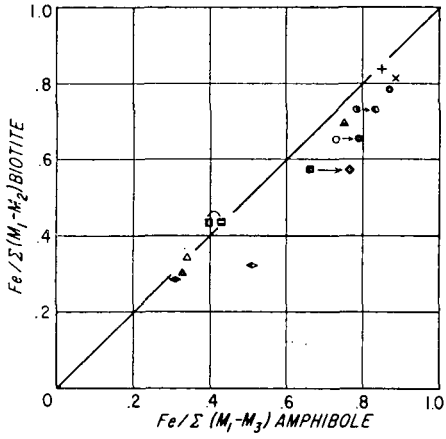

Fig. 9. Plot of $Fe/\Sigma(M_1+M_2)$ of biotite versus $Fe/\Sigma(M_1-M_3)$ of coexisting primary amphibole for rocks of the Pliny Range.

in the two phases are not supported by the Pliny Range analyses. Indeed, cogent arguments have been made both by Gorbatschev (1970) and Hazen and Wones (1972) concerning the necessity for high Fe contents in biotites to be balanced by high Al^{IV} contents in order that the tetrahedral layers and octahedral layers might better articulate. In the Pliny Range amphiboles and biotites Fe/(Fe+Mg) partitioning is not related to Al^{IV} (or $(Al+Fe^{+3})^{IV}$), nor is Ti^{+4} related to these variables. Although the octahedral M_1-M_3 sites in amphibole are similar to the M_1 and M_2 sites in biotite, the tetrahedral sites are quite different.

K_D values for the distribution of Mn and Ti between amphibole and biotite are listed in table 8. Moxham (1965), Kretz (1959), Greenland, Gottfried, and Tilling (1968), and Czamanske and Wones (1973) have shown that Mn is preferentially concentrated in amphibole. The values of K_D calculated for the Pliny Range samples are typical and seem to support the suggestion of Greenland, Gottfried, and Tilling that high values of K_D may reflect rapid cooling and a "freezing" of K_D at a higher temperature. Specifically, K_D values for the syenites are lowest, commensurate with the possibility of their recrystallization, whereas the average K_D value for the White Mountain Magma Series is 1.90, similar to that found by Greenland, Gottfried, and Tilling for the Tatoosh pluton and the Jemez Mountain volcanics.

There is no consistent change in the K_D for Mn relating to formation of the secondary amphiboles, a fact explained by the tolerance of the amphibole structure for Mn^{+2}, and the lack of a "sink" for Mn^{+2} with lower chemical potential. Mn content of amphibole and biotite correlates weakly with Fe/(Fe+Mg), and the mafic phases in the granitic rocks tend to be highest in Mn.

As is typical (for example, Kretz, 1959; Moxham, 1965; and Czamanske and Wones, 1973), Ti^{+4} is enriched in biotite relative to amphibole

for the Pliny Range rocks (table 8). Czamanske and Wones have interpreted this as a reflection of the less constrained structure of biotite. Excluding data relating to the demonstrably secondary amphiboles 46_2, 166_2, and 171_2, the average value of K_D^{Ti} is 0.47. Notable reduction in the TiO_2 content of the secondary amphiboles has produced significantly lower values for K_D^{Ti}. We suggest that, in contrast to the situation for Mn, secondary amphibole and biotite (for example, Moore and Czamanske, 1973) will typically be depleted in Ti^{+4} because of the stability of sphene and rutile.

INTENSIVE PARAMETERS DURING CRYSTALLIZATION OF THE PLINY RANGE ROCKS

We have attempted to reconstruct the conditions of crystallization of the Pliny Range magmas in terms of the intensive parameters: temperature, pressure, H_2O fugacity, O_2 fugacity, and HF fugacity. In intrusive rocks, the minerals used to estimate intensive parameters typically undergo varying amounts of reequilibration subsequent to their crystallization. The extent of reequilibration varies among different mineral species and for different mineral equilibria and may depend on rock permeability.

Temperature.—Feldspar equilibria provide a first estimate of crystallization temperature. From consideration of the alkali feldspar solvus (Waldbaum and Thompson, 1969), the alkali feldspar in the hastingsite quartz syenite, which is the least potassic (table 1), must have crystallized at a temperature in excess of 650°C. In comparison, the most potassic alkali feldspars, as found in the coarse syenite and Conway granite, could have crystallized, or recrystallized, at a temperature as low as 550°C.

Seck (1971) has determined the distribution of albite molecule between plagioclase and alkali feldspar as a function of temperature. This method of temperature determination has merit in that zoned plagioclase yields a continuous record of crystallization. A defect is that the alkali feldspar may not preserve its magmatic composition. On the basis of Seck's data, Stormer (1975) has developed numerical methods for the "Barth Thermometer." Feldspar crystallization temperatures calculated according to this system are presented in the lower part of figure 10. (Note that there is no significance to the vertical stacking of these estimates in fig. 10, where they have been presented for ready comparison with other means of temperature estimation.) With the exception of the quartz monzodiorite, in which the plagioclase shows extreme zoning from An_{54} cores to An_{23} rims, coexisting feldspars in the Pliny Range rocks indicate equilibration temperatures of 540° to 740°C.

Another means of temperature determination is through the use of coexisting magnetite–ilmenite pairs (Buddington and Lindsley, 1964). The three rocks that contain oxide pairs that show some possibility of reflecting magmatic temperatures are diorite, hastingsite quartz syenite, and Conway granite. Following Mazzulo, Dixon, and Lindsley (1975), we assumed $MnTiO_3$ to be inert and calculated oxide equilibration tempera-

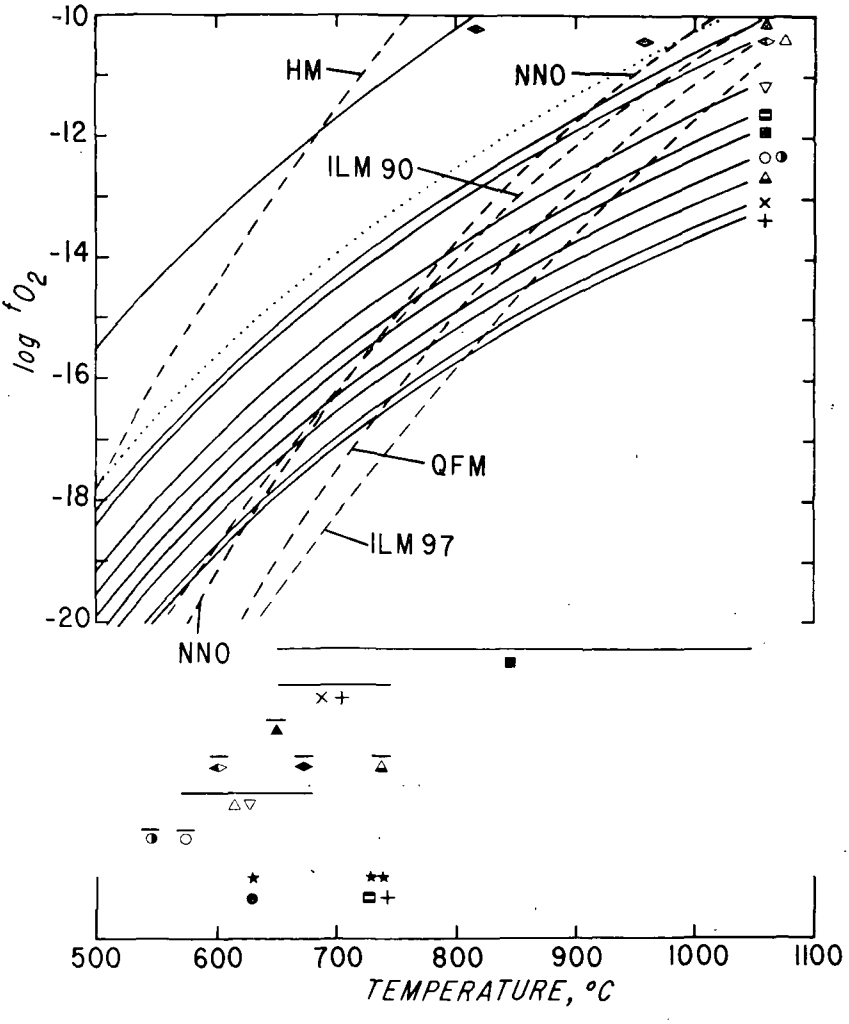

Fig. 10. Plot of log f_{O_2} versus temperature in °C for biotites of the Pliny Range, calculated at f_{H_2O} = 2 kb. (Dotted line for uncorrected curve for medium-grained syenite; see text.) Dashed curves are for the assemblages $Fe_3O_4+Fe_2O_3$, HM: Ni+NiO; $Fe_3O_4+SiO_2+Fe_2SiO_4$, QFM; $spinel_{ss}+Ilm_{90}hm_{10}$, ILM_{90}; and $spinel_{ss}+Ilm_{97}hm_3$, ILM_{97}. Solid bars below represent temperatures calculated from coexisting feldspars. Stars near temperature axis represent temperatures calculated from coexisting Fe-Ti oxides. Symbols for all data as in heading of table 4.

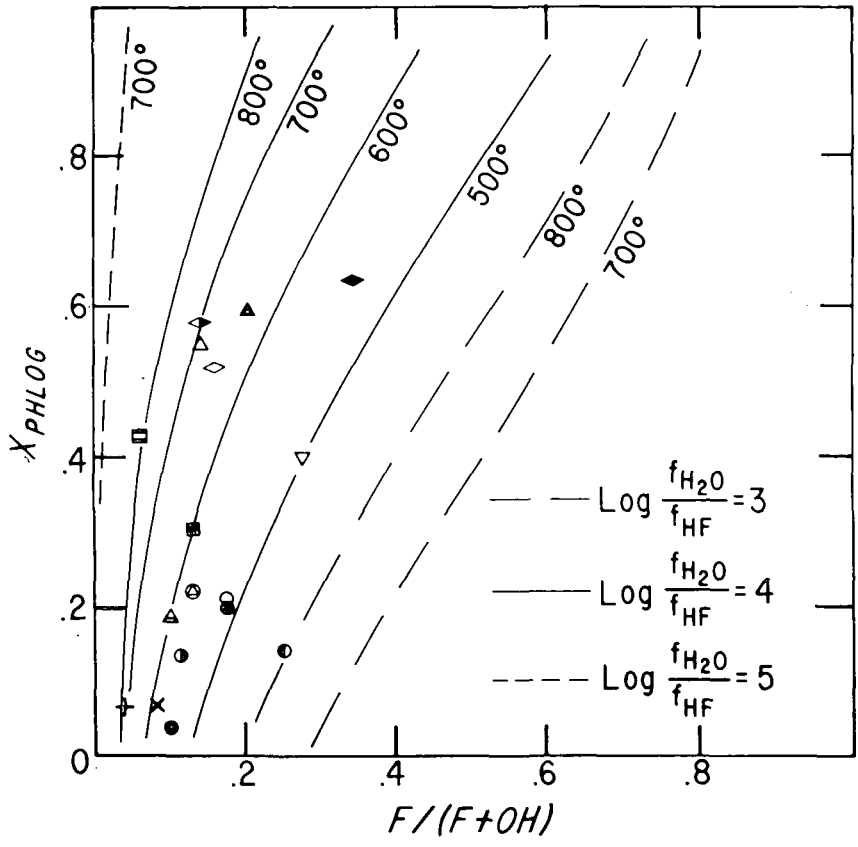

Fig. 11. Plot of Mg^{+2}/Σ oct. versus F/(F+OH) for biotites of the Pliny Range. Temperatures in °C (see Munoz and Ludington, 1974).

tures for these units of, respectively, 730°, 740°, and 630°C at oxygen fugacities of 10^{-16} to $10^{-18.7}$ atm. Temperatures estimated from the other pairs are less than 600°C.

Oxygen fugacity, H_2O fugacity, and temperature plots.—Geologic evidence and mineralogic indicators may be used to estimate total pressure and H_2O fugacity during magmatic crystallization. The presence of miarolitic cavities and pegmatitic textures is commonly taken to indicate that a magma was saturated with a gaseous phase at the time of emplacement (Burnham and Jahns, 1962). On the basis of this criterion, one may assume that a vapor phase coexisted with the quartz monzodiorite, the hastingsite quartz syenite, the pink biotite granite, and the hastingsite granite.

Assuming that H_2O was the dominant species in the gas phase coexisting with the Pliny Range magmas, an estimate of total pressure provides a value for H_2O fugacity during crystallization. The total pressure in each magma was a function of the thickness of host rock cover at the

time of intrusion. Construction of a volcanic edifice as a surface expression of magmatism could have caused substantial variation in total pressure during the course of evolution of the intrusive complex. The position of the Al_2SiO_5 triple point during Acadian metamorphism in New England is 30 to 40 km southwest of the Pliny Range (Thompson and Norton, 1968). Using a regional pressure gradient based on metamorphic assemblages across New England, we suggest that the Pliny Range magmas were intruded at pressures less than 3 kb, unless a very thick section of volcanic deposits was built up over the range during the period of intrusive activity.

Tuttle and Bowen (1958) first showed that the composition of a silicate melt coexisting with quartz, alkali feldspar, and gas indicates total pressure (fig. 12). Understanding of the crystallization of granitic rocks was increased by determination of melt compositions in anhydrous systems (Luth, 1969), in An-bearing systems (James and Hamilton, 1969), as a function of pressure (Luth, Jahns, and Tuttle, 1964), and as a function of H_2O content (Whitney, 1975; Steiner, Jahns, and Luth, 1975). The granitic magmas of the Pliny Range contained about 3 percent normative An (table 2), and some apparently became water-saturated during crystallization. The pink biotite granite contains miarolitic cavities and is the best candidate for a rock that crystallized quartz throughout its solidification history. Water saturation presumably occurred after a significant part of the magma had solidified. Consideration of figure 12 suggests that this rock crystallized at a total pressure of 2 to 3 kb.

On the basis of the two lines of evidence outlined above, we have selected a value of 2 kb as the upper limit of the fugacity of water during final crystallization of the Pliny Range magmas. This value is compatible with the estimate by Wilson (1969) that the WMMS intrusive rocks at Ossipee Lake were emplaced under a load of 1.5 to 2 kb.

Having chosen a value for f_{H_2O}, it is now possible to proceed with yet another means of estimating temperature and f_{O_2} during magmatic crystallization. Essential ingredients are: (1) the aforementioned data of Buddington and Lindsley (1964) for the Fe–Ti oxides, (2) the data of Wones and Eugster (1965) and Wones (1972) for biotite, and (3) the results of R. W. Charles and D. R. Wones (unpub.) which show that the equilibrium, sphene + magnetite + quartz + ilmenite + hedenbergite, lies at oxygen fugacities slightly higher than those of Ni–NiO. Because sphene, magnetite, and quartz are found in most of the rock units in the complex (table 1), the Ni–NiO curve of figure 10 is of great importance and may be taken as a lower limit to the f_{O_2} that prevailed during crystallization.

Calculation of the mole fraction $Fe_2O_3/(Fe_2O_3+FeTiO_3)$, assuming that $MnTiO_3$ is inert, shows that all except one of the units contain ilmenite ranging between Ilm_{90} and Ilm_{97} (table 7). Stability curves for these compositions (Buddington and Lindsley, 1964) are plotted on figure 10. The biotite stability data of Wones and Eugster (1965) and Wones

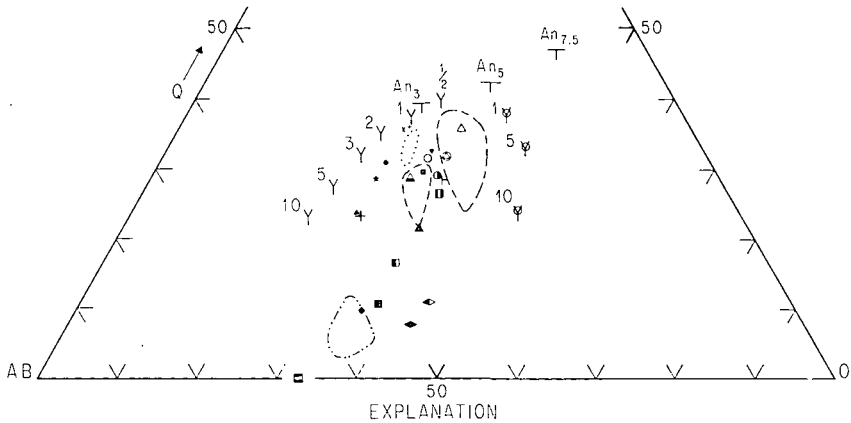

Pliny Range Units
- Conway granite (171)
- Hastingsite biotite granite (169)
- Pink biotite granite (115)
- Granite porphyry (34)
- Hastingsite quartz syenite (SK)
- Porphyritic quartz monzonite (78)
- Quartz monzodiorite (70)
- Diorite (W)
- Medium-grained syenite (119)
- Coarse syenite (177)

White Mountain Magma Series Unit
- Riebeckite granite (41)
- Conway granite
- Mt. Osceola granite (39)
- Mt. Lafayette granite porphyry (38)
- Mt. Garfield porphyritic quartz syenite (34)
- Albany quartz syenite (32)

Finnmarka Unit
- Finnmarka granite

Nigerian Younger Granite Units
- Albite riebeckite granite
- Riebeckite granite
- Biotite granite
- Amphibole granite
- Syenite

Pikes Peak Batholith Fields
- ····· Mount Rosa riebeckite granite
- – – Fayalite-free granite
- – – – Fayalite granite
- —·· Quartz syenite

Reference symbols
- ^{5}Y Ternary minimum, $P_{H_2O}=P_{TOTAL}$ (P in kilobars)
- An_3 Ternary minimum, $P_{H_2O}=P_{TOTAL}=1$kb (An in percent)
- ^{5}☿ Ternary minimum, $P_{H_2O}=0$ (P in kilobars)

Fig. 12. Projection of bulk compositions of Pliny Range rocks onto the Qz + Ab + Or ternary. Pliny Range rocks are compared to those of the Nigerian Younger Granites (Jacobsen, MacLeod, and Black, 1958); the Pikes Peak batholith (Barker and others, 1975); Finnmarka (Czamanske, 1965); and other WMMS intrusive rocks (Billings and Wilson, 1964; numbers following units are from their table 14). Ternary minima for various compositions and pressure conditions as referenced in the text.

(1972) can be used to generate intersections in f_{O_2}–T space with the stability curves for Ni–NiO and ilmenite. Biotite stability curves drawn in figure 10 are calculated for the chosen H_2O fugacity of 2 kb. Annite mole fractions were taken as the fraction of Fe^{+2} in the octahedral site as this variable is used for biotite solution models (Wones, 1972). The curves are not markedly sensitive to H_2O fugacity; a shift from 2 to 1 kb moves them only 0.6 log unit with respect to f_{O_2}. Because biotites are stable at f_{O_2} values below their stability curves and sphene–magnetite–quartz assemblages are stable only above Ni–NiO, the maximum temperatures of crystallization for each rock unit are indicated by the intersection of the appropriate biotite stability curve with the Ni–NiO curve.

Indicated maximum temperatures of crystallization range between 910°C for the porphyritic quartz monzonite and 625°C for the hastingsite quartz syenite.

In light of the preceding analysis, the Ilm_{90} and Ilm_{97} stability curves plot in positions that are anomalously rich in $FeTiO_3$ molecule with respect to probable f_{O_2} or T during crystallization. The calculated hematite mole fractions of table 7 are seen to be relatively independent of $MnTiO_3$ content, and "raw" ilmenite values (table 7) range between Ilm_{46} and Ilm_{89}. These considerations suggest that $MnTiO_3$ cannot be ignored as an ilmenite component, and that the application of the data of Buddington and Lindsley to manganiferous ilmenites in intrusive rocks must await additional experimental work. The relations in figure 10 support the contention that manganiferous ilmenites are stable at higher oxygen fugacities than manganese-free ilmenites (see Czamanske and Mihálik, 1972).

The presence of well-crystallized hematite in the medium-grained syenite suggests that biotite crystallization in that rock may have been buffered by the hematite–magnetite assemblage, perhaps during metamorphism by the younger intrusives. This suggestion is supported by the fact that the refractive index of the biotite is high for its total Fe-content, implying oxidation. The work of Wones and Eugster (1965) and Wones, Burns, and Carroll (1971) shows that this biotite should have deficiencies in both Fe^{+2} and OH^{-1}, through auto-oxidation by a loss of hydrogen. On the basis of their data, our estimate of Fe^{2+}/Σ oct. for the biotite was revised, generating a preferred f_{O_2}–T curve for the biotite in the medium-grained syenite (fig. 10). This curves lies at higher values of f_{O_2} because a greater proportion of the total iron is assumed to be in the ferric state. The intersection of this revised biotite stability curve and the hematite–magnetite buffer curve is at about 670°C, in good agreement with the feldspar equilibration temperature for this unit (fig. 10).

The mineral assemblages in these rocks change with time, and our analysis succeeds only in describing points in a changing regime. Presumably each magma began as a water undersaturated melt with or without phenocrysts and, through cooling, followed some particular T–P–f_{H_2O}–f_{O_2} path. We have suggested that pressure is invariant at less than 2 kb. We have assumed that f_{H_2O} builds up as the melt crystallizes anhydrous minerals, until it reaches some maximum value which, because of the properties of H_2O, must be less than the total pressure. The f_{O_2}–T path followed by each magma (or its derivative rock unit) may be: (1) a function of the melt and its fractionation path, (2) a function of the interaction of the melt with gas or inclusions containing oxidizing or reducing species, or (3) buffered by its own internal mineral assemblage.

We have suggested that the medium-grained syenite and pink biotite granite have been oxidized, perhaps during the release of magmatic volatiles, followed either by differential loss of H_2 and H_2O or by the addi-

tion of oxidizing ground water. In the other rocks, the f_{O_2}–T path may be buffered. In figure 10 it can be seen that the biotite curves are much shallower than the oxide curves. In rocks with relatively few opaque oxides and much biotite, we would expect that the oxides might re-equilibrate on cooling, and that biotite would define the f_{O_2}–T path. In rocks with little biotite, but containing sphene, magnetite, amphibole, ilmenite, and quartz, we would expect the f_{O_2}–T path to follow approximately the Ni–NiO buffer curve, with late crystallization of iron-rich biotite. Thus, in the quartz monzonite, pink biotite granite, and granite porphyry, we find recrystallization of magnetite, but in the hastingsite quartz syenite the biotite crystallized late by reaction of perthite and oxides and replacement of amphibole.

f_{H_2O}/f_{HF} ratios.—Munoz and Ludington (1974) demonstrated that the f_{H_2O}/f_{HF} ratio of a coexisting gas phase can be estimated from the F content of a given biotite, if its Mg content is known. Figure 11 is a plot of F/(F+OH) versus $X_{phlogopite}$ for the Pliny Range biotites; contours are drawn for selected temperatures at three fixed values of f_{H_2O}/f_{HF}. Considering our previous temperature estimates, it seems probable that log f_{H_2O}/f_{HF} was about 4 during crystallization at the Pliny Range, although continued reaction of the biotite with vapor during subsolidus cooling would result in OH-enrichment in the biotite. Ludington (1974) has found that a value of 4 for log f_{H_2O}/f_{HF} is common in many igneous rocks. When estimates of crystallization temperature are taken into account, there is no simple system or sequence to the Pliny Range magmas in terms of f_{H_2O}/f_{HF}. The very F-rich magmas of the Nigerian granitic rocks (Borley and Frost, 1963) are in contrast to those of the Pliny Range.

Conclusions concerning intensive parameters.—There is no simple relation between the intensive parameters of the Pliny Range magmas. The individual magmas appear to have been discreet entities with different H_2O and HF contents that crystallized at about 2 kb pressure. Some of the magmas appear to have coexisted with a gas phase for a considerable time; the quartz monzodiorite appears to have become saturated at a late stage in its development. The feldspar compositions in most units appear to have equilibrated at or near magmatic temperatures. Crystallization temperatures similar to those obtained from the feldspars result from consideration of biotite stabilities in rocks containing the assemblage sphene + magnetite + quartz. Variations in apparent crystallization temperature, f_{O_2}, and f_{H_2O}/f_{HF} make systematic evolution through differentiation or assimilation difficult to accept for the Pliny Range intrusive sequence.

BULK ROCK AND MINERAL CHEMISTRY

The Pliny Range rocks fall into four natural groups. The syenites and the late granitic stocks are established as groups by clear-cut age and structural style considerations (fig. 2). Between these two, two additional groups are based on the chemical discontinuity between the mafic central stock and ring dike and the granitic ring dikes. This separation is clearly

shown in figure 4 in which these units are plotted as histogram bars of areal outcrop percentage versus SiO_2 content. Data summarized in figure 2 show that whole-rock Fe/(Fe+Mg) progresses from lower to higher values in only three cycles, because the granitic ring dikes do not constitute a cycle distinct from the two mafic units. The chemistry of the primary amphiboles and biotites suggests magmatic equilibrium between these two phases in each of the Pliny Range intrusive units (for example, fig. 9).

The first intrusive group, the Pliny Range syenites, has the "mildly alkaline" character that Chapman (1968) finds typical of WMMS syenites: they have higher contents of Al_2O_3 and significantly lower Na/(Na+K) than comparable rocks (Billings and Wilson, 1964; Jacobsen, MacLeod, and Black, 1958; Oyawoye, 1969; and Barker and others, 1975). Rock analyses (table 2) show that the two older syenites are almost indistinguishable. Both units have undergone a weak deformation and metamorphism. Analyses of the mafic silicates strongly suggest that amphibole and biotite in the medium-grained syenite crystallized under substantially more oxidizing conditions than those in the coarse syenite (compare Czamanske and Wones, 1973). Bulk rock Fe/(Fe+Mg) is greater and CaO is lower in the medium-grained syenite than in the coarse syenite. These data imply that the medium-grained syenite magma was more fractionated; it may also have had a higher H_2O content and reached H_2O saturation earlier in its crystallization. Oxidation related to the release of that H_2O would explain the difference in oxidation state of the two syenites.

Diorite and quartz monzodiorite comprise the second rock grouping. The quartz monzodiorite, though possessing a higher Fe/(Fe+Mg) as might be expected for a more differentiated rock, is one of the two most reduced rocks analyzed in terms of Fe^{+3}/Fe^{+2}. The presence of rounded inclusions of coarse syenite in the quartz monzodiorite, the indication from mapping that it was intruded into coarse syenite, and its conspicuous affinity to the diorite suggest that the quartz monzodiorite may have originated through assimilation of coarse syenite into a ring dike of dioritic magma. Calculations show that the major-element chemistry of the quartz monzodiorite is closely approached by a mixture of 72 percent diorite and 28 percent coarse syenite. However, the fluorine chemistry of the micas (see fig. 11), R.E.E. chemistry (Loiselle, personal commun., 1976) and the relative oxidation states show conclusively that this is not a tenable hypothesis.

The hastingsite quartz syenite of the third group has the second highest observed value of Fe^{+3}/Fe^{+2} and the highest Fe/(Fe+Mg) value. It shows the most extreme contrast of any unit between rock oxidation state (table 2) and Fe/(Fe+Mg) for amphibole and biotite. Bulk rock chemistry (table 2) shows unequivocally that this is a highly differentiated rock. The high iron content and iron-rich mafic phases are typical of a highly oxidized, late-stage magma. The relatively large amount of modal

magnetite that has preserved a composition characteristic of magmatic conditions reinforces this conclusion. Field relations show that only the granitic rocks are younger, and this syenite seems unique among the Pliny Range rocks in having no close affinities to any of the earlier or later rock types. Consideration of modal analyses (table 1) suggests that the hastingsite quartz syenite may be related to the porphyritic quartz monzonite by a process of alkali feldspar accumulation. Alkali feldspar and plagioclase compositions in the two rocks are similar, the essential difference in the modes being that the hastingsite quartz syenite contains approximately twice the alkali feldspar and half the plagioclase.

The prophyritic quartz monzonite has identical SiO_2; higher Al_2O_3, MgO, and CaO; and lower total iron, Na_2O, and Fe^{+3}/Fe^{+2} than the hastingsite quartz syenite. It could be related to the pink biotite granite and the granite porphyry, which have higher SiO_2 and Fe/(Fe+Mg) and lower Al_2O_3, total iron, and CaO. However, the porphyritic quartz monzonite contains a more sodic plagioclase (table 1) than either of these possible derivatives and has a similar area of outcrop than either the granite porphyry or hastingsite quartz syenite. Hence, the porphyritic quartz monzonite may have developed independently of these other units. The porphyritic quartz monzonite and the pink biotite granite (especially sample 94), two units that are intimately related in space (fig. 1) and time (fig. 2), contain amphibole and biotite that have Fe/(Fe+Mg) ratios unusually low for rocks from a magmatic ring complex. The porphyritic quartz monzonite is similar to the granite in the Finnmarka complex in which the biotite has a similar Fe/(Fe+Mg). By analogy (compare, Czamanske and Wones, 1973) and considering bulk rock Fe^{+3}/Fe^{+2} for these units, the evidence is compelling that oxidation was an important process in the evolution of these two magmas.

On the basis of bulk chemistry and Fe/(Fe+Mg), the pink biotite granite and granite porphyry are quite similar rocks. The pink biotite granite is the matrix of an igneous breccia that contains pegmatitic zones and miarolitic cavities indicative of a volatile-rich melt. The smaller size and complex origin of the pink biotite granite apparently combined to promote concentration of a fluid phase that caused oxidation and a distinctly higher Fe^{+3}/Fe^{+2}, as compared to the granite porphyry. It is possible that incorporation of meteoric water was also involved in this oxidation process. Fe^{+3}/Fe^{+2} for the bulk rock and Fe/(Fe+Mg) for the mafic silicates indicate that the granite porphyry is a significantly more reduced rock. If the three units are genetically related, the granite porphyry may have preserved a lower Fe^{+3}/Fe^{+2} and relatively more reduced mafic silicate compositions because of its substantial mass.

The hastingsite biotite granite and the Conway granite of the fourth group have Fe^{+3}/Fe^{+2} and Fe/(Fe+Mg) ratios for bulk rock and mafic silicates typical of granitic rocks associated with ring complexes. Their bulk chemistry is quite similar to that of the pink biotite granite and granite porphyry.

Consideration of data from other magmatic ring complexes (Billings and Wilson, 1964; Jacobsen, MacLeod, and Black, 1958; Oyawoye, 1969; Barker and others, 1975; Czamanske, 1965) in terms of Fe^{+3}/F^{+2} suggests that such complexes may evolve with little change in rock Fe^{+3}/Fe^{+2} — Zarandah, Pikes Peak, and other WMMS rocks — or with increasing Fe^{+3}/Fe^{+2} — Younger Granite Province of Nigeria and Finnmarka. The Pliny Range rocks are unique in the wide range of Fe^{+3}/Fe^{+2} represented. There is no regular trend in bulk rock Fe^{+3}/Fe^{+2}, and Fe/(Fe+Mg) for the Pliny Range rocks and minerals also shows uniquely wide and irregular variation.

Models for magmatic ring complexes (for example Jacobsen, MacLeod, and Black, 1958; Chapman, 1966 and 1968; and Barker and others, 1975) suggest that complexities such as fractional crystallization, reaction melting, and floored polymagmatic chambers are all involved in the evolution of these complexes. It is perhaps less surprising that the Pliny Range is so complex than that other ring complexes have seemed so chemically simple.

ORIGIN AND DISTINCTIONS OF THE PLINY RANGE ROCKS

The extensive discussion of Barker and others (1975), based in part on Upton's (1960) perceptive paper on the alkaline igneous complex at Kûngnât Fjeld, is so relevant to the Pliny Range that we will only attempt to relate the geology of New Hampshire to their modeling. Chapman and Williams (1935) found it difficult to explain the WMMS on the basis of simple magmatic differentiation and concluded that fractional crystallization, assimilation, and selective fusion each were involved in producing the WMMS. Modell (1936), in his study of the Belknap Mountains, found difficulty in producing large volumes of free quartz in the end-stage rocks. He favored a "palingenetic action" (Holmes, 1931) and perceptively noted that, "the magma resulting from fusion of the crustal rocks must have been reacted upon, to a considerable extent, by the magma of the ascending cupola, for the chemical composition of the silica-rich intrusives is not unrelated to the previous intrusions, ..." Greenwood (1951), in suggesting a process to account for the comparable features of the Younger Intrusives of Nigeria and the WMMS, also envisioned a modified, palingenetic partial melting of felsic crustal constituents by a gabbroic magma. Laurent and Pierson (1973) in their study of alkaline WMMS rocks from Vermont demonstrated that two separate magma systems exploited a common conduit. They argued for partial melting of the upper mantle as the source of the feldspathoid- and quartz-bearing syenites.

Barker and others, Upton, and Chapman and Williams all present theories of origin that begin with a quiescent pool of alkali olivine basalt magma roofed by rocks of the lower crust. The generation of that magma is open to question, but several lines of evidence indicate that deep-seated, mantle-related processes have been involved in the evolution of the WMMS. Chapman (1968) has concisely presented the case that WMMS

rocks lie in a well-defined belt, with regular distribution of the plutonic centers. Recently, Foland and Faul (1977) have determined ages of intrusion for nearly all the WMMS intrusives. Their data, showing periodicity of intrusion at 230 m.y., 200 to 156 m.y., and 125 to 100 m.y., are consistent with hypothesis that the intrusions are emplaced along a zone of wrench faulting which may be the extension of an oceanic fracture (Ballard and Uchupi, 1972 and 1975; Fletcher, Sbar, and Sykes, in press.) Fletcher, Sbar, and Sykes report evidence that the fracture zone is roughly coincident with a seismic zone characterized by negative P-wave traveltime residuals, evidence permissive of the presence of basalt in the lower crust. It is intriguing that a similar picture of periodic intrusion and a major lithospheric fracture has emerged from South American-African lineaments (Marsh, 1973).

The diversity of magma types represented in the Pliny Range must have originated in a more complex crustal section than that invoked by Barker and others for the Pikes Peak batholith. There, the lower crust was assumed to be "of granulite facies mineralogy and largely depleted of its original granitic fraction, whereas the intermediate crust was of amphibolite facies and contained the roots of both calc–alkalic and peraluminous batholiths." Similar preparation of the crust had taken place throughout much of New Hampshire, for Billings (1956) concludes that the Highlandcroft and New Hampshire plutonic events preceded the WMMS.

The Pliny Range is situated within the Bronson Hill anticlinorium, a unique structural feature in New Hampshire. The anticlinorium is relatively free of the muscovite-bearing, peraluminous quartz monzonites of middle to late Paleozoic age which intrude the regions on either side and contains most of the granodioritic and quartz dioritic intrusive rocks of the Northern Appalachians. We suggest that, at the beginning of the Mesozoic, the crustal section from which the Pliny Range magmas were to evolve was more inhomogeneous than that of much of New England and could produce a uniquely complex intrusive sequence by partial fusion at different crustal levels.

Special features of the Pliny Range include extensive development of early syenite, the large areal exposure of central diorite, marked variations in whole-rock Fe^{+3}/Fe^{+2} and mafic phase Fe/(Fe+Mg), the absence of alkali amphibole and olivine, the occurrence of plagioclase as an abundant modal phase, and the relatively small amount of Conway granite.

Upton's (1960) model for the origin of the Kûngnât syenites relies predominantly on palingenesis in deep crustal areas, whereas that of Chapman (1968) relies more heavily upon melting (presumable "reaction-melting" à la Barker and others) at levels higher in the crust. White Mountain syenites differ from those of similar association in having consistently lower Na/(Na+K), and the Pliny Range syenites are high in Al_2O_3 and low in total iron. We speculate that, in comparison with the

Pikes Peak and Kûngnât syenites, the Pliny Range syenites evolved by reaction at multiple crustal levels.

In comparison with other magmatic ring complexes, the coherent central mass of diorite in the Pliny Range is unusual. It precedes the granitic rocks, forms the core of the complex, and, even excluding the quartz monzodiorite, accounts for 34 percent of the outcrop area of the undeformed rocks (fig. 4). Modell (1936) has described a comparable early central mass of WMMS diorite in the Belknap Mountains, which is shattered and veined by two later WMMS units. The gabbro ring dike that follows the syenites at Kûngnât is considered by Upton (1960) to be an advanced fractionation product of the olivine basalt magma and is a much more primitive rock. We suggest that the diorite evolved by renewed reaction-melting of alkali olivine basalt, or a derivative thereof, with crustal rocks. If this reaction takes place in the intermediate crust, the modeling of Barker and others (1975), embellished by the polymagmatic concepts of Chapman (1969), would allow the dioritic and granitic magmas to evolve concurrently. It seems quite essential that the magmas form independently, considering the marked chemical discontinuity between the two rocks groups.

The absence of alkali amphibole suggests that the magmas of the Pliny Range were less differentiated than comparable complexes or were derived from a more aluminous source. The absence of fayalite in these rocks is compatible with the observation of Jacobsen, MacLeod, and Black (1958) that, in more slowly cooled, coarser grained porphyries and granites, "fayalite has generally been converted into amphibole and biotite."

Creasy (1974) bases much of his fractionation scheme for the White Mountain batholith on crystallization of feldspar and finds only microperthite in all rock units other than the Conway granite. Oyawoye (1969) and Upton (1960) found insignificant amounts of plagioclase in the syenites of Nigeria and Kûngnât. The Pliny Range rocks provide a marked contrast to these several examples, as plagioclase is abundant in each unit (table 1). Creasy interpreted decreases in the Al_2O_3 content of biotite and in the Al_2O_3 and CaO contents of ferrohastingsite to result from fractional crystallization of feldspar. These effects, which presumably precede the evolution of alkali amphiboles, have not been noted in the Pliny Range. Corroborating this line of reasoning is the fact that the Nigerian ferrohastingsites, which are so similar to those of the Pliny Range, come from rocks that are early in the intrusive cycle (Borley, 1973). Reflecting the unusual range of rock types and oxidation states, the Pliny Range hastingsites have a greater range of composition than found by Creasy (1974) or Borley and Frost (1963).

We suggest that in many magma chambers throughout New Hampshire, reaction melting during the Mesozoic was so regular that it produced chemically indistinguishable Conway granite (Frye, 1965). In areas where middle and late Paleozoic plutonic events had partially fused and

depleted the crust in Al_2O_3 and H_2O, the Conway granite may be a dominant WMMS rock type. We suggest that in the Pliny Range, within the unique setting of the Bronson Hill anticlinorium, it was only after generation of early Mesozoic magmas by partial fusion that a crustal region mature enough to produce Conway granite was created. The tectonic setting evidently evolved as well, for the pattern of caldera subsidence and ring dike formation was followed, with the Conway granite and hastingsite biotite granite, by resurgence with the emplacement of stocks (see Smith and Bailey, 1968).

Although the initial Sr^{87}/Sr^{86} of the Conway granite is relatively low (0.705; Foland, Quinn, and Giletti, 1971), a significant crustal component in the granite is not ruled out because the crust was relatively young. Some of the proposals and alternatives which have been considered could be resolved by systematic Sr-isotope and R.E.E. studies.

Appendix

Thin section description of rock units

Coarse syenite: The dominant perthite phenocrysts up to 2 cm in length show highly irregular grain boundaries and are embayed and replaced by matrix minerals; rarely, they have cores of An_{50} plagioclase. Plagioclase phenocrysts are weakly zoned with a range in anorthite content of a few percent. Irregular quartz grains to 3 mm long are interstitial to the feldspar. The felsic minerals in the matrix are equigranular, with grain sizes typically 0.1 mm or less; myrmekite is sometimes found in the larger grains of the matrix.

A metamorphic, recrystallization texture is strongly suggested by the mafic silicate, matrix constituents of samples 147 and 155. In 147, fresh biotite is a conspicuous element in intergranular areas and replaces perthite to a minor extent. This biotite (pleochroism: buff to clear, light brown) typically consists of mats of shreds down as small as 0.05 mm but may occur as laths up to 1 mm in length. Amphibole was not noted. In contrast, sample 155 contains substantially less biotite but has striking intergrown laths of fresh amphibole up to 1 mm in length (pleochroism: pale yellow to blue-green). These laths commonly contain rounded quartz inclusions to 0.03 mm. Sample 178 shows little evidence of microgranulation and recrystallization, has the most altered mafic minerals, and shows development of epidote, sericite, and calcite. (There is substantially less alteration in samples 147 and 155.) Amphibole grains up to 1 mm contain abundant, rounded quartz inclusions. Only traces of biotite are present, most biotite having been replaced by chlorite. Chlorite, with anomalous blue interference colors, also has replaced amphibole at grain margins. All three samples contain conspicuous sphene in grains as large as 2 x 3 mm.

Medium-grained syenite.—The medium-grained syenite is similar to the coarse syenite except that the perthite phenocrysts range only up to 3 mm in length. Contacts between perthite phenocrysts are more common in this syenite and are highly irregular and interlocking, with the suggestion of late albite migration. Plagioclase compositions are more variable than those of the coarse syenite. The felsic components of the matrix of sample 138 tend to be of even finer grain size than those in the coarse syenite, although some interstitial quartz grains may be 0.5 mm across. Biotite is the most abundant mafic silicate in 138 and occurs as disseminated flakes up to 0.15 mm long or occasionally as clots of flakes which may measure 1.5 mm across. The texture suggests recrystallization. Only incipient alteration to chlorite was noted. There is minor, irregular amphibole (<0.4 mm across) in sample 138. Sphene is conspicuous in the medium-grained syenite as bullet-shaped grains to 0.9 mm long that include quartz, biotite, and opaque oxides.

Diorite.—In diorite specimen W, a diabasic texture is dominated by plagioclase laths averaging under 1 mm in length, whereas the quartz monzodiorite (46) possesses a granitic texture characterized by grains to 3 mm, with a significant fraction of perthite and quartz. Plagioclase in both units is zoned from cores of $An_{50\pm5}$ to rims of $An_{23\pm2}$. Perthite has crystallized later than plagioclase, and quartz is clearly interstitial. The diorite is considerably altered to chlorite, sericite, and epidote.

Although some pyroxene is altered to amphibole, the rock contains numerous subhedral grains of fresh pyroxene (to 0.8 mm long), and pyroxene comprises 5.7 percent of the rock. In contrast, pyroxene in the quartz monzodiorite occurs only as corroded cores in a few amphibole grains. Amphibole (pleochroism: buff to light brown) and biotite (pleochroism: pale buff to reddish brown) in W occur as extremely irregular crystals up to 2 mm across. Much of the amphibole does not contain pyroxene inclusions and, because it contains small plagioclase inclusions, must have crystallized contemporaneously with plagioclase. Because biotite is anhedral, it is not clear what proportion of the biotite is primary and what portion has replaced amphibole. Sample W contains over 7 volume percent chlorite which has formed after biotite.

Quartz monzodiorite.—In specimen 46, amphibole and biotite occur as compact, individual grains to 1.5 mm across or as intergrown clusters of grains. The dominant amphibole (pleochroism: buff to olive) is irregularly replaced by a later amphibole (pleochroism: buff to blue-green). Biotite (pleochroism: light straw to medium brown) occurs in grains to 1.5 mm which are clearly primary. Minor biotite replaces both types of amphibole. In both the diorite and quartz monzodiorite, the opaque oxides occur as abundant, small, embayed grains (0.1 to 0.4 mm), suggestive of corrosion or resorption.

Hastingsite quartz syenite.—The hastingsite quartz syenite of specimen 164 consists predominantly of perthite (to 3 x 5 mm), rounded quartz grains to 2 mm across, and fresh laths of amphibole to 1.5 mm long. In contrast specimen 163 contains over 20 percent plagioclase. Internally, many of the perthite grains have areas up to 0.7 mm across composed of feathery, feldspar intergrowths similar to granophyric texture and of different optical orientation to the host. Contacts between perthite grains are typically not sutured, in contrast to other WMMS units.

The large, fresh amphibole grains (pleochroism: light tan to bright yellow) are intergrown with fine-grained quartz and perthite, frequently contain inclusions of these minerals to 0.2 mm across, and have an interstitial aspect, all of which suggests that amphibole crystallized late. The entire unit is remarkably poor in biotite (table 1), and only a few small grains of somewhat altered biotite (pleochroism: pale brown to greenish brown) to 0.2 mm long are present in 163 and 164. The optical properties suggest a high ferric iron component.

Porphyritic quartz monzonite.—Specimen 85 consists dominantly of a nearly equigranular, coarse intergrowth of plagioclase, perthite, and quartz. Conspicuous in the rock are fine-grained (0.1 to 0.4 mm) interstitial areas composed of these minerals and the mafic phases as well as highly complex, recrystallized contacts between feldspars. Texturally, the rock is similar to samples of the hastingsite biotite granite (166, 174, and 175) and quite distinct from the Conway granite (82 and 171). The rock is slightly altered, with development of sericite, epidote, and chlorite. Perthite grains to 3 x 5 mm are common and, in contrast to other units, show microcline grid twinning; the perthite is typically cloudy but contains clear patches of twinned albite (to 0.2 mm). Plagioclase occurs as grains to 3 mm in length and quartz to more than 2 mm across.

Biotite (pleochroism: nearly colorless to pale brown) occurs as irregular, embayed grains to 0.6 mm across but is typically finer (to 0.2 mm) as scattered grains and small aggregates. Amphibole (pleochroism: light straw to pale, yellowish green) is smaller in grain size (0.01 mm) and sparse. Sparse chlorite is present in the rock, and clusters of epidote (to 0.6 mm across) and ilmenite are common.

Pink biotite granite.—The predominant texture in specimens 94 and 114 is allotriomorphic-granular, with interlocking grains of perthite, quartz, and plagioclase. This texture is especially well shown by 94 in which the average grain size of 60 percent of the rock is 0.1 to 0.3 mm with the remainder comprised of irregular perthite and quartz grains to 0.9 mm across. Specimen 114 is somewhat coarser, with a matrix of grains averaging perhaps 0.5 mm and irregular, interstitial quartz grains to 2 mm across.

Specimen 114 contains scattered biotite grains to 0.5 mm across and a greater abundance of chlorite grains which have totally replaced biotite (pleochroism: pale buff to medium brown). The chlorite has plum-colored birefringence. Small clusters of epidote and opaque oxide grains may mark the sites of former amphibole, but none is present in the rock now. Specimen 94 contains more abundant, fresher biotite (pleochroism: very pale yellow to medium brown) scattered through the fine-textured rock in grains 0.1 to 0.4 mm across. Minor alteration to chlorite is present. Minor,

fresh amphibole (pleochroism: pale straw to pale yellowish green) occurs as grains averaging 0.1 mm across. The amphibole may occur as isolated grains or in association with aggregates of fine biotite. Minor sphene is present in association with mafic mineral clusters. Allanite is present in small quantities in both specimens.

Granite porphyry.—The texture of the granite porphyry is very distinctive because of the presence of a felsic "droplet" texture. Perthite grains to 3 mm in length, rounded, resorbed quartz grains to 2.4 mm, and plagioclase grains to 1 mm comprise the phenocrysts. Interstitial to these grains and distributed through many of the feldspar grains are fine, rounded quartz and orthoclase grains in the size range 0.02 to 0.1 mm. Whereas the centers of large perthite grains are commonly free of inclusions, they often contain random and semi-linear strings of inclusions near grain boundaries. Creasy (ms) has observed similar features in the Mt. Osceola and Conway granites of the White Mountain batholith. Smaller perthite and plagioclase grains are often riddled with inclusions. Quartz phenocrysts display highly irregular, resorbed margins and commonly contain marginal chains of small "corrosion" holes. This texture is more typical of that commonly displayed by shallow porphyry intrusive bodies than the texture of any other unit in the Pliny Range.

Amphibole (pleochroism: buff to olive) in the granite porphyry occurs as irregular, poikilitic grains to 0.6 mm across and is somewhat altered along margins and cleavages to an unidentified, reddish orange, isotropic phase. Biotite (pleochroism: straw to deep, greenish brown) is also irregular in outline, poikilitic, and of similar dimensions to the amphibole. Microprobe analysis (table 4) reveals no clue to this phenomena, a fact that indirectly supports the presumption (compare Deer, Howie, and Zussman, 1962) that the unusual pleochroism may reflect an unusually high ferric iron content. Chlorite replaces biotite and lesser amounts of amphibole. Rare, poikilitic grains of allanite to 0.7 mm long are present.

Hastingsite biotite granite.—The three specimens (166, 174, and 175) of hastingsite biotite granite have similar allotriomorphic to hypidiomorphic granular textures. Perthite and quartz grains may range up to 3 x 5 mm in 175 but more commonly are in the range 1 to 3 mm. Plagioclase cores are occasionally found in the perthite grains. The perthite is coarse, with small, twinned patches of albite. Contacts between perthite grains may be complex and sometimes are marked by small grains of exsolved (?) albite. Quartz is interstitial and irregular.

Specimens 174 and 175 contain no amphibole grains suitable for analysis, although scattered amphibole remnants are found in biotite in 175. Biotite (pleochroism: pale buff to medium brown) occurs in all three rocks as grains to 1.5 mm across (typically 0.8 mm). In all specimens, biotite is somewhat altered to chlorite along cleavages, and, in 174, some biotite grains are fully replaced by chlorite (pleochroism: buff to light olive). Specimen 166 contains two amphiboles which are partly replaced by biotite. The older amphibole (pleochroism: greenish buff to light, olive green) occurs in grains to 1 x 1 mm but is extensively replaced by a younger amphibole (pleochroism: pale, olive green to blue-green). Zoned subhedral to euhedral allanite crystals to 0.7 mm long are typical of this unit.

Conway granite.—Specimens 82 and 171 are fresh rocks which display dominantly hypidiomorphic-granular texture; coarse perthite to 3 x 5 mm, quartz grains to 2 mm across, and plagioclase grains 2 mm long are typical. Contacts between perthite grains are slightly sutured and show evidence of late albite migration, but in comparison to other granitic units the rock texture is clean and uncomplicated, similar to that of the Madoc, Ontario granite (Tuttle and Bowen, 1958, pl. 2). The albitic phase of the perthite commonly shows twinning. Plagioclase may occur as cores in perthite, indicating that it began to crystallize early.

The mafic assemblages in specimens 82 and 171 differ in appearance, although the phases in the two rocks are chemically similar (tables 3 and 4). In 82, fresh amphibole (pleochroism: light brown to olive green) occurs as irregular grains (to 6 mm across) which are interstitial to perthite and quartz. Late crystallization of amphibole is common in rocks of the White Mountain batholith (Creasy, ms) and in the Younger granite province of Nigeria (Jacobsen, MacLeod, and Black, 1958). Figure 14 of Jacobsen, MacLeod, and Black shows a texture identical to that seen in the Conway granite of the Pliny Range. Biotite (pleochroism: pale straw to reddish brown) occurs in trace amounts as grains to 0.15 mm long. In 171, large (to 1.5 mm across), primary, single crystals of biotite (pleochroism: straw to dark brown) commonly occur interstitially. Only a few small grains (to 0.5 mm) of amphibole are present in the rock and, in further contrast to 82, are typically altered to biotite plus quartz. Small amounts of allanite are present in the Conway granite.

REFERENCES

Anderson, A. T., 1968, Oxidation of the LaBlache Lake titaniferous magnetite deposit, Quebec: Jour. Geology, v. 76, p. 528-547.

Ballard, R. D., and Uchupi, E., 1972, Carboniferous and Triassic rifting: A preliminary outline of the tectonic history of the Gulf of Maine: Geol. Soc. America Bull., v. 83, p. 2285-2302.

———— 1975, Triassic rift structure in Gulf of Maine: Am. Assoc. Petroleum Geologists Bull., v. 59, p. 1041-1072.

Barker, F., Wones, D. R., Sharp, W. N., and Desborough, G. A., 1975, The Pikes Peak batholith, Colorado Front Range, and a model for the origin of the gabbro-anorthosite–syenite–potassic granite suite: Pre-Cambrian Geology, v. 2, p. 97-160.

Billings, M. P., 1928, The chemistry, optics, and genesis of the hastingsite group of amphiboles: Am. Mineralogist, v. 13, p. 287-296.

———— 1956, The geology of New Hampshire, Pt. II. Bedrock Geology: Concord, New Hampshire State Planning and Develop. Comm., 204 p.

Billings, M. P., and Wilson, J. R., 1964, Chemical analyses of rocks and rock-forming minerals from New Hampshire, Part XIX. Mineral Resource Survey: Concord, New Hampshire, Div. Econ. Devel., 104 p.

Borg, I. Y., 1967, On conventional calculations of amphibole formulae from chemical analyses with inaccurate $H_2O^{(+)}$ and F determinations: Mineralog. Mag., v. 36, p. 583-590.

Borley, G. D., 1963, Amphiboles from the Younger Granites of Nigeria: Part 1, Chemical classification: Mineralog. Mag., v. 33, p. 358-376.

Borley, G. D., and Frost, M. T., 1963, Some observations on igneous ferrohastingsites: Mineralog. Mag., v. 33, p. 646-662.

Bowen, R. W., 1971, Graphical normative analysis program (Program number C542): U.S. Geol. Survey Open-file Report.

Buddington, A. F., and Leonard, B. F., 1953, Chemical petrology and mineralogy of hornblendes in northwest Adirondack granitic rocks: Am. Mineralogist, v. 38, p. 891-902.

Buddington, A. F., and Lindsley, D. H., 1964, Iron-titanium oxide minerals and synthetic equivalents: Jour. Petrology, v. 5, p. 310-357.

Burnham, C. W., and Jahns, R. H., 1962, A method for determining the solubility of water in silicate melts: Am. Jour. Sci., v. 260, p. 721-745.

Chapman, C. A., 1966, Paucity of mafic ring-dikes — evidence for floored polymagmatic chambers: Am. Jour. Sci., v. 264, p. 66-77.

———— 1968, A comparison of the Maine coastal plutons and the magmatic central complexes of New Hampshire, *in* Zen, E-an, and others, Studies of Appalachian Geology, Northern and Maritime: New York, Intersci., p. 385-396.

Chapman, C. A., Billings, M. P., and Chapman, R. W., 1944, Petrology and structure of the Oliverian magma series in the Mt. Washington quadrangle, New Hampshire: Geol. Soc. America Bull., v. 55, p. 497-516.

Chapman, R. W., 1942, Ring structures of the Pliny region, New Hampshire: Geol. Soc. America Bull., v. 53, p. 1533-1567.

Chapman, R. W., and Williams, C. R., 1935, Evolution of the White Mountain magma series: Am. Mineralogist, v. 20, p. 502-530.

Creasy, J. W., ms, 1974, Mineralogy and petrology of the White Mountain batholiths, Franconia and Crawford Notch quadrangles, New Hampshire: Ph.D. thesis, Harvard Univ.

Czamanske, G. K., 1965, Petrologic aspects of the Finnmarka igneous complex, Oslo area, Norway: Jour. Geology, v. 73, p. 293-322.

Czamanske, G. K., and Mihálik, P., 1972, Oxidation during magmatic differentiation, Finnmarka complex, Oslo area, Norway: Part I, The opaque oxides: Jour. Petrology, v. 13, p. 493-509.

Czamanske, G. K., and Wones, D. R., 1973, Oxidation during magmatic differentiation, Finnmarka complex, Oslo area, Norway: Part 2, The mafic silicates: Jour. Petrology, v. 14, p. 349-380.

Deer, W. A., Howie, R. A., and Zussman, J., 1962-1963, Rock-forming minerals, 5 v.: London, Longmans.

Eichelberger, J. C., ms, 1971, Granites and syenites of the Pliny Range, New Hampshire: M.S. thesis, Massachusetts Institute Technology, Cambridge, Mass.

Fletcher, J. P., Sbar, M. L., and Sykes, L. R., in press, Seismic trends and travel time residuals in eastern North America and their tectonic implications: Geol. Soc. America Bull.

Foland, K. A., and Faul, H., 1977, Ages of White Mountain intrusives — New Hampshire, Vermont, and Maine, USA: Am. Jour. Sci., v. 277, p. 888-904.

Foland, K. A., Quinn, A. W., and Giletti, B. J., 1971, K-Ar and Rb-Sr Jurassic and Cretaceous ages for intrusives of the White Mountain magma series, northwestern New England: Am. Jour. Sci., v. 270, p. 115-141.

Foster, M. D., 1960, Interpretation of the composition of trioctahedral micas: U.S. Geol. Survey Prof. Paper 354-B, 48 p.

Frye, J. K., ms, 1965, Composition and crystallization history of the Conway Granite of New Hampshire: Ph.D. thesis, The Pennsylvania State Univ.

Gorbatschev, R., 1969, Element distribution between biotite and Ca-amphibole in some igneous or pseudo-igneous plutonic rocks: Neues Jahrb. Mineralogie, Abh., v. 111, p. 314-342.

———— 1970, Distribution of tetrahedral Al–Si in coexisting biotite and amphibole: Contr. Mineralogy Petrology, v. 28, p. 251-258.

Greenland, L. P., Gottfried, D., and Tilling, R. I., 1968, Distribution of manganese between coexisting biotite and hornblende in plutonic rocks: Geochim. et Cosmochim. Acta, v. 32, p. 1149-1163.

Greenwood, Robert, 1951, Younger intrusive rocks of Plateau Province, Nigeria, compared with the alkalic rocks of New England: Geol. Soc. America Bull., v. 62, p. 1151-1178.

Hazen, R. M., and Wones, D. R., 1972, The effect of cation substitution on the physical properties of trioctahedral micas: Am. Mineralogist, v. 57, p. 103-129.

Holmes, A., 1931, The problem of association of acid and basic rocks in central complexes: Geol. Mag., v. 68, p. 241-255.

Jacobsen, R. R. E., MacLeod, W. N., and Black, R., 1958, Ring complexes in the younger granite province of northern Nigeria: Geol. Soc. London Mem., v. 1, 72 p.

James, R. S., and Hamilton, D. L., 1969, Phase relations in the system $NaAlSi_3O_8$–$KAlSi_3O_8$–$CaAl_2Si_2O_8$–SiO_2 at 1 kilobar water vapor pressure: Contr. Mineralogy Petrology, v. 21, p. 111-141.

Kretz, R., 1959, Chemical study of garnet, biotite, and hornblende from gneisses of southwestern Quebec with emphasis on distribution of elements in coexisting minerals: Jour. Geology, v. 67, p. 371-402.

Laurent, R., and Pierson, T. C., 1973, Petrology of alkaline rocks from Cuttingsville and the Shelburne Peninsula, Vermont: Canadian Jour. Earth Sci., v. 10, p. 1244-1256.

Leake, B. E., 1968, A catalog of analyzed calciferous and subcalciferous amphiboles together with their nomenclature and associated minerals: Geol. Soc. America Spec. Paper 98, 210 p.

Ludington, S. D., ms, 1974, Application of fluoride-hydroxyl exchange data to natural minerals: Ph.D. thesis, Univ. Colorado.

Ludington, S. D., and Munoz, J. L., 1975, Application of fluor-hydroxyl exchange data to natural micas [abs.]: Geol. Soc. America Abs. with Programs, v. 7, p. 1179.

Luth, W. C., 1969, The systems $NaAlSi_3O_8$–SiO_2 and $KAlSi_3O_8$–SiO_2 at 20 kb and the relationship between H_2O content, P_{H_2O}, and P_{total} in granitic magmas: Am. Jour. Sci., v. 267-A, p. 325-341.

Luth, W. C., Jahns, R. H., and Tuttle, O. F., 1964, The granite system at pressures of 4 to 10 kilobars: Jour. Geophys. Research, v. 69, p. 759-773.

Marsh, J. S., 1973, Relationships between transform directions and alkaline igneous rock lineaments in Africa and South America: Earth Planetary Sci. Letters, v. 18, p. 317-323.

Mazzulo, L. J., Dixon, S. A., and Lindsley, D. H., 1975, T–f_{O_2} relationships in Mn-bearing Fe–Ti oxides: Geol. Soc. America Abs. with Programs, v. 7, no. 7, p. 1192.

Modell, D., 1936, Ring-dike complex of the Belknap Mountains, New Hampshire: Geol. Soc. America Bull., v. 47, p. 1885-1932.

Moore, W. J., and Czamanske, G. K., 1973, Compositions of biotites from unaltered and altered monzonitic rocks in the Bingham Mining district, Utah: Econ. Geology, v. 68, p. 269-274.

Moxham, R. L., 1965, Distribution of minor elements in coexisting hornblendes and biotites: Canadian Mineralogist, v. 8, p. 204-240.

Munoz, J. L., and Ludington, S. D., 1974, Fluoride-hydroxyl exchange in biotite: Am. Jour. Sci., v. 274, p. 396-413.
Naylor, R. S., 1969, Age and origin of the Oliverian domes, central western New Hampshire: Geol. Soc. America Bull., v. 80, p. 405-427.
Neiva, A. M. R., 1976, The geochemistry of biotites from granites of northern Portugal with special reference to their tin content: Mineralog. Mag., v. 40, p. 453-466.
Nockolds, S. R., 1947, The relation between chemical composition and paragenesis in the biotite micas of igneous rocks: Am. Jour. Sci., v. 245, p. 401-420.
Oyawoye, M. O., 1969, The geology of the Zarandah ring complex, northern Nigeria: Jour. Min. Geol. (Nigeria), v. 3, p. 33-47.
Page, L. R., 1968, Devonian plutonic rocks in New England, *in* Zen, E-an, and others, eds., Studies of Appalachian Geology, Northern and Maritime: New York, Intersci., p. 371-383.
Robinson, Peter, Ross, M., and Jaffe, H. W., 1971, Composition of the anthophyllite–gedrite series, comparisons of gedrite–hornblende, and the anthophyllite–gedrite solvus: Am. Mineralogist, v. 56, p. 1005-1041.
Seck, H., 1971, Koexistierende alkalifeldspäte und plagioklase in system $NaAlSi_3O_8$–$KAlSi_3O_8$–H_2O bei temperaturen von 650°C bis 900°C: Neues Jahrb. Mineralogie, Abh., v. 115, p. 315-345.
Simonen, A., and Vorma, A., 1969, Amphibole and biotite from rapakivi: Bull. Comm. Geol. de Finlande, no. 238, 28 p.
Smith, R. L., and Bailey, R. A., 1968, Resurgent cauldrons, *in* Studies in Volcanology: Geol. Soc. America Mem. 116, p. 613-662.
Smith, R. L., and Ross, C. S., 1961, Structural evolution of the Valles Caldera, New Mexico, and its bearing on the emplacement of ring dikes: U.S. Geol. Survey Prof. Paper 424-D, p. 145-149.
————1970, Geologic Map of the Jemez Mountains, New Mexico: U.S. Geol. Survey Misc. Geol. Inv. Map I-571.
Steiner, J. C., Jahns, R. H., and Luth, W. C., 1975, Crystallization of alkali feldspar and quartz in the haplogranite system $NaAlSi_3O_8$–$KAlSi_3O_8$–SiO_2–H_2O at 4 kb: Geol. Soc. America Bull., v. 86, p. 83-98.
Stormer, J. C., 1975, A practical two-feldspar geothermometer: Am. Mineralogist, v. 60, p. 667-674.
Thompson, J. B., 1947, Role of aluminum in the rock forming silicates [abs.]: Geol. Soc. America Bull., v. 58, p. 1232.
Thompson, J. B., and Norton, S. A., 1968, Paleozoic regional metamorphism in New England and adjacent areas, *in* Zen, E-an, and others, eds., Studies of Appalachian Geology, Northern and Maritime: New York, Intersci., p. 319-327.
Tuttle, O. E., and Bowen, N. L., 1958, Origin of granite in light of experimental studies: Geol. Soc. America Mem. 74, 142 p.
Upton, B. G. J., 1960, The alkaline igneous complex of Kûngnât Fjeld, South Greenland: Midd. Grøn., v. 123, p. 1-29.
Waldbaum, D. R., and Thompson, J. B., 1969, Mixing properties of sanidine crystalline solutions; IV. Phase diagrams from equations of state: Am. Mineralogist, v. 54, p. 1274-1298.
Whitney, J. A., 1975, The effects of pressure, temperature, and X_{H_2O} on phase assemblage in four synthetic rock compositions: Jour. Geology, v. 83, p. 1-31.
Wilson, J. R., 1969, The Geology of the Ossipee Lake Quadrangle, New Hampshire: New Hampshire Dept. Res. and Econ Development Bull. 3, 116 p.
Wones, D. R., 1972, Stability of biotite: a reply: Am. Mineralogist, v. 57, p. 316-317.
Wones, D. R., Burns, R. G., and Carroll, B. M., 1971, Stability and properties of synthetic annite: EOS, Am. Geophys. Union Trans., v. 52, p. 369-370.
Wones, D. R., and Eugster, H. P., 1965, Stability of biotite: experiment, theory, and application: Am. Mineralogist, v. 50, p. 1228-1272.